

AttackBench: Evaluating Gradient-based Attacks for Adversarial Examples

Antonio Emanuele Cinà^{*§}, Jérôme Rony^{†§}, Maura Pintor^{‡x}, Luca Demetrio^{*x},
Ambra Demontis[‡], Battista Biggio^{‡x}, Ismail Ben Ayed[†], Fabio Roli^{*‡}

^{*}University of Genoa [†]ÉTS Montréal [‡]University of Cagliari ^xPluribus One

Email: ^{*} antonio.cina@unige.it, [†] jerome.rony.1@etsmtl.net,

arXiv:2404.19460v1 [cs.LG] 30 Apr 2024

Abstract—Adversarial examples are typically optimized with gradient-based attacks. While novel attacks are continuously proposed, each is shown to outperform its predecessors using different experimental setups, hyperparameter settings, and number of forward and backward calls to the target models. This provides overly-optimistic and even biased evaluations that may unfairly favor one particular attack over the others. In this work, we aim to overcome these limitations by proposing AttackBench, *i.e.* the first evaluation framework that enables a fair comparison among different attacks. To this end, we first propose a categorization of gradient-based attacks, identifying their main components and differences. We then introduce our framework, which evaluates their effectiveness and efficiency. We measure these characteristics by (i) defining an *optimality* metric that quantifies how close an attack is to the optimal solution, and (ii) limiting the number of forward and backward queries to the model, such that all attacks are compared within a given maximum query budget. Our extensive experimental analysis compares more than 100 attack implementations with a total of over 800 different configurations against CIFAR-10 and ImageNet models, highlighting that only very few attacks outperform all the competing approaches. Within this analysis, we shed light on several implementation issues that prevent many attacks from finding better solutions or running at all. We release AttackBench as a publicly-available benchmark, aiming to continuously update it to include and evaluate novel gradient-based attacks for optimizing adversarial examples.

Index Terms—Evasion attacks, benchmark, computer vision

I. INTRODUCTION

Machine-learning models are employed in countless domains of applications, including pedestrian segmentation [1], malware detection [2], and biometric identity recognition [3]. However, such models are vulnerable to adversarial examples, carefully-crafted inputs that force the target model to make erroneous decisions at test time [4], [5]. Given the growing popularity of machine learning, we witness a proliferation of attacking strategies, all claiming to be the best so far in terms of success rate. These attacks are often computed through gradient descent algorithms that minimize a loss function of choice to find suitable adversarial perturbations in a fast and efficient way. Due to the large variety of developed attacks, many recent works propose extensive evaluations against several models [6]–[8] to understand their effectiveness. However, none of these focus on ranking the efficacy of attacks, but they rather evaluate robustness of machine learning models. To exacerbate the problem, these techniques have

been tested under unfair settings, and understanding the performance of these attacks remains difficult due to the lack of standardized protocols for comparing them. In particular, most techniques are tested against various sets of machine learning models, not shared among different evaluations, test data and settings, like different numbers of iterations. Furthermore, attacks exhibit different performance depending on the tuning of their hyperparameters. This choice impacts the quality of the computed adversarial examples, hindering the comparison of different attacks. Lastly, most attacks have been re-implemented several times without guaranteeing their correctness and consistency with the original implementations, causing many recent evaluations to overestimate the robustness of the proposed defense mechanisms [9].

For these reasons, we propose AttackBench: a unified benchmark that fairly tests adversarial attacks under the same assumptions, not correlated to a fixed perturbation budget. First, we propose a general categorization that expressively captures all the proposed adversarial attacks, thus showing that most are similar or almost identical. Then, we re-evaluate these attacks by executing them in a consistent experimental setup. We consider a benchmark setup that launches the attacks against the same machine learning models, using the same test data and the same amount of computational budget for each. Consequentially, we devise a novel metric named *optimality* to rate and rank the attacks effectively. Under the same initial conditions and across multiple runs, our metric rates each attack by comparing the resulting adversarial examples with all the other attacks included in the benchmark.

We perform an extensive experimental analysis that compares 20 attacks (listed in Table I), retrieving their original implementation and collecting the other implementations available among popular adversarial attack libraries. We empirically test a total of 102 techniques, re-evaluating them in terms of their runtime, success rate and perturbation distance, as well as with our newly introduced *optimality* metrics. While implementing our benchmark, we collected additional insights, including sub-optimal implementations, attacks returning incorrect results, and errors in the source code that prevent attacks from concluding their runs correctly. These additional insights could lead to a complete re-evaluation of the State of the Art, as incorrect evaluations might have impacted and inflated results in published work. To foster reproducible results, we open source

[§]Equal contribution

AttackBench and provide all the results on online leaderboard,¹ thus providing a service for researchers of new attacks to easily assess the performance of their developed strategies and compare them with the others in unified settings.

We summarize our findings as follows:

1. We develop a categorization of adversarial attacks, recasting all the existing techniques inside a unified framework (Sect. II);
2. we propose AttackBench, a consistent and fair evaluation benchmark for adversarial attacks that evaluates them on the same models, data, and computational budget (Sect. III);
3. we propose the novel *optimality* metric, which fairly ranks adversarial attacks based on the quality of adversarial examples they produce (Sect. III-B);
4. we extensively test 102 attacks and we rank them according to our novel metric (Sect. IV);
5. we highlight 5 programming errors inside the code of some attacks we have considered, and we present inconsistent results of different implementation of the same attack (Sect. IV).

II. GRADIENT-BASED ATTACKS

We present here an original categorization of gradient-based attacks on machine-learning models that unifies different formulations in the literature (Sect. II-A), and then discuss the main limitations present in current attack evaluations and comparisons (Sect. II-B).

A. Attack Categorization

Summarized in Table I, our categorization is defined by (i) the attack type and the perturbation constraints, (ii) the loss function optimized by the attack, (iii) the initialization strategies, (iv) the descent direction used by the attack to update the perturbation in each iteration, (v) the optimization algorithm, and (vi) the scheduling policy for annealing the step size during the optimization. We present each of these aspects in the following sections.

1) *Minimum-norm vs Fixed-budget Attacks*: Let us assume, without loss of generality, that the input samples lie in a d -dimensional (bounded) space, *i.e.* $\mathbf{x} \in [0, 1]^d$, and that their labels are denoted with $y \in \{1, \dots, C\}$. Then, the predicted label of a trained model parameterized by θ can be denoted with $\hat{y} = f(\mathbf{x}, \theta)$, while the confidence value (logit) for class c can be denoted with $f_c(\mathbf{x}, \theta)$ and the softmax-rescaled logits with $z_c(\mathbf{x}, \theta)$. The predicted label can thus be computed also as $\hat{y} = \arg \max_c f_c(\mathbf{x}, \theta)$. Under this setting, we argue that finding an adversarial example amounts to solving the following multi-objective optimization:

$$\underset{\delta}{\text{minimize}} \quad (L(\mathbf{x} + \delta, y; \theta), \|\delta\|_p), \quad (1)$$

$$\text{subject to} \quad \mathbf{x} + \delta \in [0, 1]^d, \quad (2)$$

where $L(\mathbf{x} + \delta, y; \theta)$ is a loss defining the misclassification objective, and δ is the perturbation optimized to find an adversarial example $\mathbf{x}' = \mathbf{x} + \delta$ within the feasible domain. The loss function L defines the objective of the attack so that L is large when the input is correctly classified, whereas it is lower when the model predicts a wrong label for \mathbf{x} .²

¹<https://attackbench.github.io>

²For targeted attacks, one can minimize $L(\mathbf{x} + \delta, y_t; \theta)$, being $y_t \neq y$ the label of the target class.

Comparing the loss function used here to that used when training machine-learning models, they achieve opposite goals. The second objective in Eq. 1 is expressed as a constraint on the size of the perturbation $\|\delta\|_p$, formulated through the usage of ℓ_p norms. Commonly used perturbation norm constraints are $\ell_0, \ell_1, \ell_2, \ell_\infty$, that produce respectively sparse to increasingly dense perturbations. The constraint in Eq. 2 is a box constraint that ensures the sample remains within the input space of the model, *i.e.* $\mathbf{x} + \delta \in [0, 1]^d$.

The optimization problem expressed in Eq. 1 presents an inherent tradeoff: minimizing L favours the computation of adversarial examples with large misclassification confidence, but also a large perturbation size, whereas minimizing $\|\delta\|_p$ penalizes larger perturbations (in the given ℓ_p norm) at the expense of decreasing the misclassification confidence.

Multi-objective problems like Eq. 1 can be solved by establishing a trade-off between the given objectives along the Pareto frontier by optimizing one objective and using the other as a constraint. Consequently, we can find two main families of attacks, where one aims at finding the inputs that cause the maximum error within a given perturbation budget (fixed-budget attacks), and the counterpart that searches for the smallest perturbation needed to achieve misclassification (minimum-norm attacks).

Fixed-budget Attacks. We call a first group fixed-budget attacks (`FixedBudget`), which minimize the loss and set the perturbation size as the constraint. They optimize the following problem:

$$\underset{\delta}{\text{minimize}} \quad L(\mathbf{x} + \delta, y, \theta), \quad (3)$$

$$\text{subject to} \quad \|\delta\|_p \leq \epsilon, \quad (4)$$

$$\mathbf{x} + \delta \in [0, 1]^d, \quad (5)$$

where $\|\cdot\|_p$ indicates the ℓ_p -norm operator. The loss L in the objective of Eq. 3 is a loss function approximating the classification outcome, defined accordingly to the goal of the attack, *i.e.* untargeted or targeted misclassification. For example, this group of attacks include Projected Gradient Descent (PGD) [16].

Minimum-norm Attacks. these attacks (`MinNorm`) minimize the size of the perturbation and set the misclassification on the model as a constraint. They are formulated as follows:

$$\underset{\delta}{\text{minimize}} \quad \|\delta\|_p \quad (6)$$

$$\text{subject to} \quad f(\mathbf{x} + \delta, \theta) \neq f(\mathbf{x}, \theta), \quad (7)$$

$$\mathbf{x} + \delta \in [0, 1]^d, \quad (8)$$

where $\|\cdot\|_p$ indicates the ℓ_p -norm operator. However, this problem cannot be solved directly by gradient descent since the misclassification constraint (7) is not differentiable.

There are two ways to solve this problem. The first solution adopts the `FixedBudget` formulation for different values of ϵ , by applying heuristics to minimize the norm of the perturbation (like enlarging or shrinking ϵ during the computations, as done by Decoupling-Direction-Norm (DDN) [18], and the Fast Minimum-Norm (FMN) [26] attacks). The other solution consists of transforming the constrained problem into an unconstrained one, by using a differentiable relaxation of

TABLE I: List and categorization of earlier adversarial attacks, and of the attacks considered in our evaluation benchmark.

Name	Attack Type	Norms				Descent Direction	Optimizer	Step size (α) Scheduler	Loss L	Init δ_0
		ℓ_0	ℓ_1	ℓ_2	ℓ_∞					
Biggio et al. [4] (2013)	FixedBudget		✓	✓		Grad	GD	–	$f_y(\mathbf{x}; \theta)$	Zero
Szegedy et al. [5] (2014)	MinNorm				✓	Grad	L-BFGS-B	–	NCE	Zero
FGSM [10] (2015)	FixedBudget				✓	Proj	GD	–	NCE	Zero
JSMa [11] (2015)	MinNorm	✓				Proj	GD + Mom	–	$z_y(\mathbf{x}; \theta)$	Zero
BIM [12] (2016)	FixedBudget				✓	Proj	GD	–	NCE	Zero
DeepFool [13] (2016)	MinNorm			✓		Norm	GD	–	DL	Zero
CW [14] (2017)	MinNorm	✓		✓	✓	Grad	Adam	–	DL	Zero
EAD [15] (2018)	MinNorm		✓	✓	✓	Grad	GD	Poly	DL	Zero
PGD [16] (2018)	FixedBudget			✓	✓	Proj	GD	–	NCE	Zero
BB [17] (2019)	MinNorm	✓	✓	✓	✓	Proj	L-BFGS-B	Lin	DL	Adv
DDN [18] (2019)	MinNorm			✓		Norm	GD	Cos	NCE	Zero
PGD- ℓ_0 [19] (2019)	FixedBudget	✓				Proj	GD	–	NCE	Zero
SparseFool [20] (2019)	MinNorm		✓			Norm	GD*	–	DL	Adv
TrustRegion [21] (2019)	MinNorm			✓	✓	Grad	GD	–	DL	Zero
FAB [22] (2020)	MinNorm		✓	✓	✓	Proj	GD	RoP	DL	Random
APGD [23] (2020)	FixedBudget			✓	✓	Proj	GD + Mom	RoP	NCE/DLR	Zero
ALMA [24] (2021)	MinNorm		✓	✓		Grad	RMSProp + Mom	Exp	DLR	Zero
APGD- ℓ_1 [25] (2021)	FixedBudget		✓			Proj	GD + Mom	RoP	DLR	Zero
FMN [26] (2021)	MinNorm	✓	✓	✓	✓	Norm	GD	Cos	DL	Any
PDGD [27] (2021)	MinNorm			✓		Proj	Adam	Lin, Exp	DL	Zero
PDPGD [27] (2021)	MinNorm	✓	✓	✓	✓	Prox	Adam	Lin, Exp	DL	Zero
VFGA [28] (2021)	MinNorm	✓				Grad	GD*	–	$z_y(\mathbf{x}; \theta)$	Zero
σ -zero [29] (2024)	MinNorm	✓				Norm	Adam	Cos	DL	Zero

the constraint (7), *e.g.*, the difference between the output score of the original class y and the scores of the other classes, and adding it to the objective as a penalty component, with an appropriate trade-off parameter. For instance, the Carlini-Wagner attack (CW) [14] implements the following objective: $\min_{\delta} \|\delta\|_p + c \cdot \min(L(\mathbf{x} + \delta, y, \theta), -\kappa)$, where c controls the trade-off between the misclassification objective and the perturbation size. However, these penalty methods are slow in practice (c requires a search). Thus, an Augmented Lagrangian Method for Adversarial (ALMA) attacks [24] has been proposed to adaptively adjust the trade-off between the norm minimization objective and the misclassification constraint, by leveraging penalty-Lagrangian functions.

In contrast to FixedBudget attacks, which maximize confidence for predicting a wrong class within a given perturbation budget, MinNorm attacks aim at finding the closest adversarial example to each input. This requires solving a more complex problem, as it amounts not only to finding a valid adversarial example, but also to minimizing its perturbation size [24].

Solution Algorithm. We describe here a generalized attack, given as Algorithm 1, which encompasses the main steps performed by most of the FixedBudget and MinNorm attacks. The attack starts by initializing the perturbation (line 1), and then iterates K times. In each iteration, the attack computes the gradient of the loss function (line 4), which is processed accordingly to match norm constraints (line 5), and then it is used to tune the perturbation (line 6). Then, attacks might update their hyper-parameters (line 7). Once all the iterations have been consumed, the attack returns the best perturbation computed so far (line 8). While these steps are general, we now detail the function and the possible choices of each component used in Algorithm 1.

2) *Loss Functions:* Typically, the loss L in Eq. 1 for a gradient-based attack (line 4) is defined as $L : \mathbb{R}^d \times \mathbb{R} \rightarrow \mathbb{R}$. While early attacks used directly the y -th logit output

Algorithm 1: Generalized Attack Algorithm

Input : \mathbf{x} , the input sample; y , the class label; α , the initial step size; θ , target model; and K , the number of iterations.

Output : The adversarial example \mathbf{x}_{adv} .

```

1  $\delta_0 \leftarrow \text{init}(\mathbf{x})$  ▷ initialization
2  $\delta^* \leftarrow \delta_0, \alpha_0 = \alpha$ 
3 for  $k = 1, \dots, K$  do
4    $\mathbf{g} \leftarrow \nabla_{\delta} L(\mathbf{x} + \delta_{k-1}, y, \theta)$  ▷ loss gradient
5    $\mathbf{g} \leftarrow \text{direction}(\mathbf{g}, \alpha_k)$  ▷ descent direction
6    $\delta_k \leftarrow \text{optim}(\mathbf{x}, \delta_{k-1}, \mathbf{g})$  ▷ optimizer (proj.)
7    $\alpha_k \leftarrow \text{scheduler}(\alpha_0, k, K)$  ▷ scheduler
8  $\delta^* \leftarrow \text{best}(\delta_0, \dots, \delta_K)$  ▷ best solution
9 return  $\mathbf{x}_{\text{adv}} = \mathbf{x} + \delta^*$ 

```

of the models ($f_y(\mathbf{x}; \theta)$) [4], [5] or the y -th softmax output ($z_y(\mathbf{x}; \theta)$) [11], the majority of existing attacks now leverage the Negative Cross-Entropy (NCE) loss, the Difference of Logits (DL) [14], or the Difference of Logits Ratio (DLR) [23].

Logit and Softmax Loss. Earlier attacks, as the one proposed by Biggio *et al.* [4], and Papernot *et al.* [11] directly optimize the y -th output of the model $f_y(\mathbf{x}; \theta)$, or its softmax-scaled value $z_y(\mathbf{x}; \theta)$. The softmax outputs have recently been used also in the Voting Folded Gaussian Attack [28].

Negative Cross-entropy Loss (NCE). Firstly used by Szegedy *et al.* [5], this loss is computed as $L(\mathbf{x}, y; \theta) = \log(z_y(\mathbf{x}; \theta))$. This is basically the standard cross-entropy loss multiplied by -1 as now the goal is to *increase* the error of the model. For a targeted attack, it is sufficient to use the target label y_t instead of the true label y , and flip the sign.

Difference of Logits Loss (DL). Introduced by Carlini and

Wagner [14] in the popular attack that brings their name, this loss is directly computed with the logits, *i.e.* the outputs of the model: $L(\mathbf{x}, y; \boldsymbol{\theta}) = f_y(\mathbf{x}; \boldsymbol{\theta}) - \max_{j \neq y} f_j(\mathbf{x}; \boldsymbol{\theta})$. Assuming the classifier assigns higher scores to the correct class, the loss function takes on negative values when \mathbf{x} becomes adversarial. As for the previous case, this loss can become targeted if the score $f_t(\mathbf{x}; \boldsymbol{\theta})$ is used instead of the score for the original class, and the sign of the loss is swapped, *i.e.* the objective becomes maximizing the logit of the target class. It is worth noting that setting this loss equal to zero means finding the decision boundary, while imposing an offset means enforcing a margin of misclassification confidence on the prediction. For this reason, Carlini *et al.* [14] introduce the misclassification margin in the loss, *i.e.* $\min(L(\mathbf{x} + \boldsymbol{\delta}, y; \boldsymbol{\theta}), -\kappa)$, where κ represents the minimum distance required between the two scores.

Difference of Logit Ratio Loss (DLR). Introduced by Croce *et al.* [23], this loss function is both shift and rescaling invariant to the outputs of the model. This is obtained by using the Logit Difference Loss and dividing it by a scaling factor computed on the logits themselves as follows:

$$L(\mathbf{x}, y; \boldsymbol{\theta}) = \frac{f_y(\mathbf{x}; \boldsymbol{\theta}) - \max_{j \neq c} f_j(\mathbf{x}; \boldsymbol{\theta})}{f_{\pi_1}(\mathbf{x}; \boldsymbol{\theta}) - f_{\pi_3}(\mathbf{x}; \boldsymbol{\theta})},$$

where $f_{\pi_1}(\mathbf{x}; \boldsymbol{\theta}) \geq \dots \geq f_{\pi_c}(\mathbf{x}; \boldsymbol{\theta})$ denote the logits sorted in decreasing order. The shift invariance is achieved by applying a normalizing factor composed of a difference of top-ranking logits in the denominator.

3) *Initialization Strategies:* Some attacks perform a custom initialization to favor a better exploration of the loss landscape. Initialization can be modeled as transformations $i: \mathbb{R}^d \rightarrow \mathbb{R}^d$, and return a valid sample in the feasible domain Δ (line 1). The baseline option is to start the attack from the original point (Zero). Another option is choosing a random initialization (Random), which sets the initial estimate of $\boldsymbol{\delta}_0$ to be a random perturbation within the constraints of the optimization problem, as done by FAB [22]. Note that some attacks may also internally run the attack starting from multiple random restarts and take the best perturbation out of all trials to improve the optimization results [19]. Other attacks, like BB [17] and optionally FMN [26], can be initialized as a sample belonging to a specific target class (Adv), and minimize the perturbation by getting closer and closer to \mathbf{x} during the iterations.

4) *Descent Directions:* To speed-up the optimization, attacks use different strategies that modify the gradient in each iteration before passing it to the optimizer (line 5). We identify four main strategies to define appropriate descent directions:

1. Gradient (Grad), which uses the gradient \mathbf{g} as is;
2. Normalization (Norm), which keeps the direction of \mathbf{g} but rescales its norm to be proportional to the step size α_k in the current iteration, *i.e.*, $\mathbf{g}' = \frac{\alpha_k \mathbf{g}}{s}$, where the scaling factor is often set as $s = \|\mathbf{g}\|_p$;
3. Projection (Proj), which sets the direction by maximizing the scalar product with the gradient \mathbf{g} over an α_k -sized ℓ_p ball, as $\mathbf{g}' \in \arg \max_{\|\mathbf{v}\|_p \leq \alpha_k} \mathbf{v}^\top \mathbf{g}$;³
4. Proximal (Prox), which uses the proximal gradient [30].

³This amounts to maximizing the linear approximation of the loss function $L(\mathbf{x} + \mathbf{v}, y, \boldsymbol{\theta}) \approx L(\mathbf{x}, y, \boldsymbol{\theta}) + \mathbf{v}^\top \nabla L(\mathbf{x}, y, \boldsymbol{\theta})$ over an α_k -sized ℓ_p ball.

PGD-based attacks all use Proj, as for $p \in \{1, 2, \infty\}$ the solution can be efficiently computed in closed form. For $p = 1$, the maximum is achieved by taking the components of \mathbf{g} with maximum absolute values and setting them to $\pm \alpha_k$, according to their sign. In practice, this leads to poor performance when combined with the box constraint in Eq. 8, as it results in updating only one component in each iteration. Reformulations of this update generally include the box constraint in the maximization, *e.g.*, in ℓ_1 -APGD [23], which update the components exhibiting the largest absolute values at once, up to the box limits, until an ℓ_1 norm of α_k is achieved. For $p = 2$, the maximum is achieved when $\mathbf{g}' = \alpha_k \frac{\mathbf{g}}{\|\mathbf{g}\|_2}$, which is practically equivalent to Norm. For $p = \infty$, the maximum is achieved by setting $\mathbf{g}' = \text{sign}(\mathbf{g})$, resulting in a dense update of all components of $\boldsymbol{\delta}_k$ as in the ℓ_∞ -PGD attack [16].

5) *Optimizers:* This attack component applies the update on the current perturbation, producing a new perturbation $\boldsymbol{\delta}_k$. Optimizers are specific algorithms that implement this update, $u: \mathbb{R}^d \mapsto \mathbb{R}^d$, based on the computed gradient and a specific strategy (line 6) and return a perturbation vector of the same dimension as the input. Existing gradient-based adversarial attacks use different variants of Gradient Descent (GD), sometimes with a diagonal metric to scale different axes of the space (*e.g.* Adam (Adam)) or introducing a momentum term to avoid vanishing gradient issues (*e.g.* Momentum (GD + Mom)). Alternatively, they can use adaptive strategies where the learning rate changes over time (*e.g.* RMSprop with momentum (RMSPROP + Mom)) or second-order derivative methods (*e.g.* L-BFGS-B). Optimizers can also be combined together as in attacks that integrate linear solvers with other gradient-based sub-routine attacks (GD + LinSolv). Finally, the optimizer step might include a final projection operation that ensures the produced update $\mathbf{x} + \boldsymbol{\delta}_k$ is in the feasible domain. Specifically, it takes into account the box constraint in Eq. 1 and eventually the ε bound in Eq. 4 for the case of FixedBudget attacks.

6) *Step Size Schedulers:* Some attacks, including most of the FixedBudget attacks, use a fixed step size (-). However, as well known in optimization theory, when using GD, decreasing the step size usually leads to better convergence results. Thus, dedicated schedulers can control the optimization process. We denote them as a function $h: \mathbb{R} \mapsto \mathbb{R}$, that dynamically updates the step size α (line 7) and tune the decay to guarantee better convergence. Indeed, many attacks, especially the MinNorm, reduce the step size along the iterations, shrinking the trust region of the linear approximation (thus, the step size) to refine the solution with smaller updates as they approach the boundary. One common strategy is to use a linear step size decay (Lin), in which the step size is multiplied by a fixed amount $\gamma < 1$ at each step. Another popular scheduler is the Cosine Annealing (Cos) [31], which decays the step size gradually from a maximum value of α to a minimum of α_K . Other alternatives are exponential (Exp) or polynomial (Poly) step size decay, where the decay is controlled by an exponential descent or a specified polynomial, respectively. As another strategy, some attacks adapt the step size depending on the loss behavior over a span of iterations. In particular, when the loss plateaus for a specified number of steps, this scheduler reduces the step size by a defined factor (ROP). While these

attacks are often called *adaptive*, the term adaptive is already used in the State of the Art of adversarial attacks for denoting attacks that are customized to break a specific defense [32].

B. Limitations of Current Evaluations

In current evaluations and comparisons of gradient-based attacks, there are several limitations that we aim to address with our proposed framework. These evaluations are often conducted independently in each research paper, increasing the risk of overfitting the metrics proposed within that study and hindering reproducibility. Specifically:

1. Attacks are not re-evaluated against recent robust models;
2. FixedBudget are compared for arbitrary values of ε , whereas MinNorm generally rank attacks with the median size of perturbation, making the comparison between the two categories difficult;
3. Considered metrics are not combinable across models to reflect a global performance of the attacks ;
4. Use different datasets or subsets of points, hard to re-create;
5. Provide attacks with different computational budgets;
6. Later re-implementations of published attacks might deviate from the original ones, and these differences are often not taken into account;
7. Results are not shared, and when new attacks emerge, evaluations have to be re-run completely.

We address all these limitations with AttackBench, described in Sect. III, providing a more comprehensive and reliable evaluation framework for adversarial attacks.

III. THE ATTACKBENCH FRAMEWORK

We now describe the AttackBench framework, whose stages are conceptually depicted in Fig. 1. We detail stages (1-2) in Sect. III-A, and stages (3-4-5) in Sect. III-B, while providing insights on practical implementation details in Sect. III-C.

A. Model Zoo and Attack Benchmarking

Stage (1): Model Zoo. This stage builds a *zoo* of diverse models, encompassing robust and non-robust models, to evaluate attacks across various scenarios and minimize evaluation biases. The pool can be clearly expanded as novel defenses are released.

Stage (2): Attack Benchmarking. This stage consists of testing each attack as described in Algorithm 2, against all models in the AttackBench zoo. For each attack a (Algorithm 1), target model θ , and dataset \mathcal{D} , the algorithm returns the best minimum distances d^* found for each sample, along with the number of forward and backward queries q^* performed by the attack. We will then discuss how the best minimum distances d^* for each attack-model pair can be used to compute the corresponding *security evaluation curve*, showing how model accuracy decreases as a function of the perturbation budget ε .

Algorithm 2 starts by initializing d^* and q^* , and by wrapping the target model θ within a custom object B_θ that is used to keep track of the number of queries q^* , namely the number of forward and backward passes made by the attack to optimize each sample (line 2). The algorithm then iterates over the input

Algorithm 2: Attack Benchmarking

Input : a , the attack algorithm; θ , the target model; \mathcal{D} , the test dataset; Q , the query budget; and $p \in \{0, 1, 2, \infty\}$, the perturbation model.

Output : Min. distances d^* and required queries q^* .

```

1  $d^* \leftarrow \{\}$ ,  $q^* \leftarrow \{\}$ 
2  $B_\theta \leftarrow \text{BenchModel}(\theta, Q)$ 
3 for  $(\mathbf{x}, y) \in \mathcal{D}$  do
4    $B_\theta.\text{init\_queries}()$ 
5    $h_x \leftarrow \text{hash}(\mathbf{x})$ 
6    $\mathbf{x}_{\text{adv}} \leftarrow a(\mathbf{x}, y, B_\theta)$ 
7    $d^*\{h_x\} \leftarrow \|\mathbf{x} - \mathbf{x}_{\text{adv}}\|_p$ 
8    $q^*\{h_x\} \leftarrow B_\theta.\text{num\_queries}()$ 
9 return  $d^*, q^*$ 

```

samples \mathbf{x} and their labels y . It initializes the number of queries for the current sample to zero (line 4), and then hashes the sample (line 5) to ensure that the results are stored consistently even if the samples are loaded in batches with a different order. The attack is then run (line 6), monitoring the number of queries performed to the target model. If the query budget Q is exceeded, the attack is stopped. Whether the attack exceeds Q or not, our framework always returns the best adversarial example \mathbf{x}_{adv} found during the optimization. As pointed out in [9], this already improves many of the currently-available attack implementations that, by default, return the *last* sample (*i.e.* not necessarily the *best* one). The algorithm then computes the distance d^* between the adversarial sample \mathbf{x}_{adv} and the source sample \mathbf{x} (line 7), and retrieves the number of queries q^* spent to optimize \mathbf{x}_{adv} from B_θ (line 8). The results (d^* , q^*) for all samples are finally returned.

Design Choices. Let us highlight some relevant design choices behind the first stages of AttackBench. First, to enable adding novel attacks easily, we neither modify the code of any attack, nor change their hyperparameters. These two conditions also avoid potential misconfiguration biases. Second, we make use of an *hashing algorithm* to hash each input sample \mathbf{x} , ensuring that every evaluation considers the same conditions (see Appendix A for more details). Third, to compare attacks within a similar computational budget, we set an upper bound Q on the number of queries each attack can perform. The reason is that different attacks may perform a different number of forward and backward calls in each iteration, and some of them even query the model to improve their initialization phase. As forward and backward queries are the most computationally-demanding operations within each attack iteration [24], we use them as a fairer proxy to evaluate attack complexity, along with execution times.

Security Evaluation Curves. The so-called security evaluation curves [33], [34] show how model accuracy, denoted with $\rho(\varepsilon)$ in the following, decreases as the perturbation budget ε increases. We refer to ρ as *clean accuracy* when samples are not perturbed, *i.e.* when the perturbation budget $\varepsilon = 0$, and as *robust accuracy* when the perturbation budget $\varepsilon > 0$. The robust accuracy at a given ε corresponds indeed to the fraction of adversarial samples \mathbf{x}_{adv} that do not bypass the model,

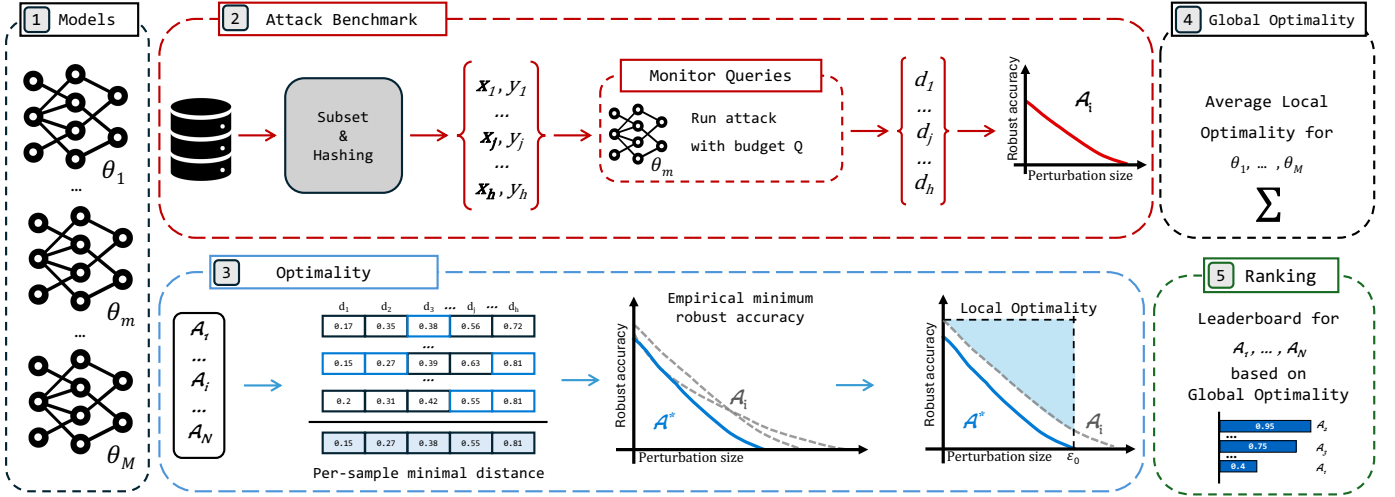


Fig. 1: A comprehensive overview of the five stages of AttackBench. Each attack is tested in fair conditions, and then it is ranked through the optimality metric. The best attack is the one that produces the higher numbers of minimally-perturbed adversarial examples with fewer queries and less time.

given that their distance to the source sample \mathbf{x} is higher than ϵ . The value of $\rho(\epsilon)$, for each attack-model pair, can be thus readily computed from the minimum distances d^* returned by Algorithm 3 as:

$$\rho(\epsilon) = \frac{1}{|\mathcal{D}|} \sum_{(\mathbf{x}, y) \in \mathcal{D}} \mathbb{I}(d_{\mathbf{x}}^* > \epsilon), \quad (9)$$

where $d_{\mathbf{x}}^*$ is the minimum-norm perturbation for the input sample \mathbf{x} , and $\mathbb{I}(\cdot)$ is the indicator function, which returns 1 if its argument is true, and 0 otherwise. By changing ϵ , one can also compute the complete security evaluation curve without any additional computational overhead. Some examples are shown in Fig. 2. It should be clear that better-performing attacks should yield security evaluation curves closer to the origin. Thus, we can define a more compact measure to evaluate the effectiveness of attacks by simply computing the Area Under the Security Evaluation Curve (AUSEC) as:

$$\text{AUSEC}_a(\epsilon_0) = \int_0^{\epsilon_0} \rho_a(\epsilon) d\epsilon, \quad (10)$$

where the subscript a identifies the underlying attack, and ϵ_0 denotes the upper bound of the integration interval, which should be set to ∞ or to the value at which $\rho(\epsilon) = 0$ to compute the complete area. We will discuss in the next section how we design a novel *optimality* metric that enables a straightforward comparison of attacks based on this AUSEC definition.

Let us conclude this section by pointing out that inspecting the complete security evaluation curve and considering AUSEC values should provide a more thorough evaluation of existing attacks and defenses. The reason is that only considering $\rho(\epsilon)$ at a fixed ϵ , as done in many evaluations and benchmarks [16], [19], [25], [35], may lead to designing attacks and defenses that just overfit that specific evaluation, yielding good results only at the most common, given ϵ , while perhaps failing when the perturbation budget slightly changes.

B. Evaluating and Ranking Attacks

The results obtained for individual attacks from Stage (2) are aggregated in the subsequent stages of AttackBench to enable a comprehensive comparison of the attacks. To this end, we define here a novel *optimality* metric, illustrated in Stage (3) of Fig. 1 and designed to evaluate the attacks' performance with a single representative value for each independent experiment (for each model θ_m). We then describe how we measure, for each attack, the global optimality score depicted in Stage (4) of Fig. 1. Finally, we conclude by presenting how new attacks can be easily integrated into the benchmark while preserving consistency in the scoring and ranking processes.

Stage (3): Optimality Score. To compare the performance of the attacks in a standardized way, thus mitigating the risk of overfitting attack performance to a single perturbation model (see Sect. II-B), we introduce the *local optimality* measure as the outcome of stage (3) of our benchmark. Unlike evaluations that solely focus on the mean [14], [15], median [17], [26], [29], [35] or arbitrary perturbation models [19], [23], [25], the optimality considers all the points of the security evaluation curve at once. We use the $\text{AUSEC}_{a^i}(\epsilon_0)$ to score each attack with one single comprehensive metric. Indeed, the area under the security evaluation curve represents the average performances of each attack considering all values of ϵ (or until ϵ_0 in practical settings in which attacks might not reach a 100% success rate). Thus, to provide an ideal upper-bound to serve as comparison, we define a^* as the attack that, for each point, returns the adversarial example computed with the least number of queries and the least perturbation, according to the considered threat model. Hence, we define $\text{AUSEC}_{a^*}(\epsilon_0)$ as the curve defined by each optimal result provided by a^* .

Local optimality (LO). To evaluate the performance of an evasion attack a^i on a specific target model θ , we define a measure that we call *LO*, denoted with ξ_{θ}^i . This metric computes the difference between the area under the curve of a^i and a^* to assess how much the first is suboptimal with respect to the

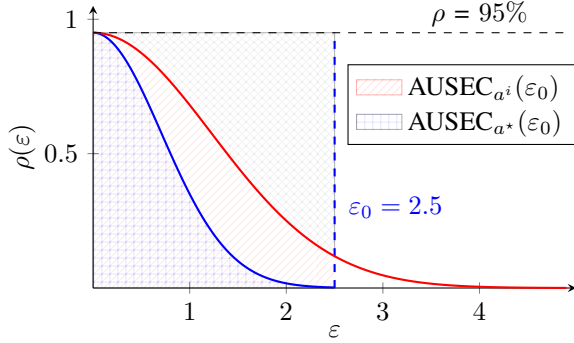


Fig. 2: Security evaluation curves of a^i and a^* .

second. Formally:

$$\xi_{\theta}^i = \frac{\rho \cdot \varepsilon_0 - \text{AUSEC}_{a^i}(\varepsilon_0)}{\rho \cdot \varepsilon_0 - \text{AUSEC}_{a^*}(\varepsilon_0)}. \quad (11)$$

In Fig. 2, we illustrate an example of the LO measure when comparing the security evaluation curve of a^i (red curve) with that of the best attack, a^* (blue curve). Notably, the highlighted area between these is non-zero, suggesting that a^i is less optimal than a^* . The adversarial examples generated by a^i thus are generally sub-optimal, *i.e.* they succeed for perturbations greater than necessary when compared to the empirical lower bound found by a^* . The box defined by $\rho \cdot \varepsilon_0$ serves to normalize the LO measure with respect to the accuracy and robustness of the target model θ . In more detail, when a target model exhibits high robustness or accuracy, it becomes inherently more challenging to evade, leading to less severe penalties for the optimality of the attack. Conversely, when the target model is more vulnerable or less accurate, the curve disparity becomes more relevant, and the impact of the attacks is more pronounced in the optimality. Furthermore, this term ensures that the LO measure is bounded in $[0, 1]$ with $\xi_{\theta}^i = 1$ when a^i performs exactly as a^* , thus finds always the smallest perturbation to evade for each sample. Conversely, when $\xi_{\theta}^i = 0$, the attack fails to find a successful perturbation with $\varepsilon \leq \varepsilon_0$, thus resulting in a curve that matches the box and therefore $\text{AUSEC}_{a^i}(\varepsilon_0) = \rho \cdot \varepsilon_0$. With this normalization, our benchmark offers a standardized scale to interpret and compare the performance of gradient-based attacks across different scenarios and models. Ultimately, the area above the red curve (cross-hatch pattern in Fig. 2) indicates the LO optimality for a^i , which is inversely proportional to the area between the red and blue curves, *i.e.* the loss in performance of a^i compared to a^* . Further details regarding the LO measure implementation are reported in Sect. B.

Stage (4): Global Optimality. While the LO measure gives a measure of the effectiveness of an attack with respect to a target model θ_m , a single value introduces the risk of overfitting to the benchmark. In fact, attacks might be developed with perfected settings to target a model θ_m but have low generalization of performance against different models. To this end, AttackBench prevents potential bias arising from the use of individual models by evaluating the attacks against a diverse set of robust models and aggregating the results to derive a global score of optimality.

Algorithm 3: Computing Local Optimality

Input : $\{a^1, \dots, a^N\}$, list of attacks for benchmark;
 \mathcal{D} , the validation dataset; θ , the target model;
 Q , query budget; p , threat model distance.
Output : Local optimality measure $(\xi_{\theta}^1, \dots, \xi_{\theta}^n)$.

- 1 **for** $a^i \in \{a^1, \dots, a^N\}$ **do**
- 2 $d_i, q_i \leftarrow \text{TestAttack}(a^i, \mathcal{D}, \theta, Q, p)$
- 3 $\rho_{\theta}^*(\varepsilon) = \text{sample-wise-min}\{d_1, \dots, d_N\}$
- 4 **for** $a^i \in \{a^1, \dots, a^n\}$ **do**
- 5 ξ_{θ}^i for attack a^i following Eq. 11
- 6 **return** $(\xi_{\theta}^1, \dots, \xi_{\theta}^n), (q_1, \dots, q_n)$

Thus, we propose another measure, namely *global optimality*, as the output of step (4) of Fig. 1.

Global Optimality (GO). The GO measure quantifies the average LO of an attack, denoted as a^i , concerning a set of target models $\mathcal{M} = \{\theta_1, \dots, \theta_M\}$. We define the GO as:

$$\xi^i = \frac{1}{|\mathcal{M}|} \sum_{\theta_m \in \mathcal{M}} \xi_{\theta_m}^i. \quad (12)$$

The GO score for an attack corresponds to the average LO measure obtained across a set \mathcal{M} of distinct models. Bounded in $[0, 1]$ as well, the GO score an attack a^i is equal to 1 only when, for each model in \mathcal{M} , a^i consistently finds the minimal adversarial perturbation that misleads all the models, thus when $a^i = a^*$ (reported as a percentage to improve readability).

Stage (5): Ranking. Lastly, AttackBench orders all the attacks using GO , grouping them according to both the perturbation they consider and the target model.

C. Implementation of the Benchmark

We provide here specific implementation details that characterize our methodology.

Hashing. AttackBench uses the SHA-512 hashing algorithm [36] to associate each sample with a unique compressed representation for accurately tracking and identifying samples throughout the benchmarking process. The choice of SHA-512 is motivated by its resistance to collisions.

Query-budget Termination. Incorporating the query-halting feature while attacks are running introduces the challenge of avoiding any intervention in their implementation. AttackBench must accept attacks as input without modifying their internal code to avoid introducing potential pitfalls that could compromise the validity of the evaluation. To overcome this challenge, we introduce a `BenchModel` class to encapsulate the models under assessment (line 2). During an attack, this class counts all the backward and forward *hooks*⁴ operations invoked on the model, without interfering with their output. Once the query limit is reached, AttackBench blocks replaces the prediction with a correct one (for an untargeted attack) in the forward pass, and zeroing the gradient in the backward pass. This ensures that the attack either can continue without causing any runtime error, even if the number of iterations surpasses the query

⁴https://pytorch.org/docs/stable/generated/torch.nn.modules.module.register_module_forward_hook.html

budget, and that the optimization is effectively halted, due to the absence of gradients. Special care was taken to ensure that these hooks are compatible with batching strategies (some samples might reach the limit before others), and do not disrupt the internal adversarial perturbation tracking mechanisms of the attack being evaluated. Ultimately, the forward and backward hooks implemented by AttackBench track the progress of adversarial example optimization and save the best adversarial perturbation found. This approach addresses the issue identified by Pintor *et al.* [9], who demonstrated that certain attack implementations return the adversarial perturbation from the last iteration, even though it may not be the best perturbation found during optimization. Thus, within AttackBench, we ensure to report the best-case performance of the attacks.

Including New Attacks into the Benchmark. AttackBench facilitates the inclusion of new attacks thanks to three main characteristics. First, AttackBench treats attacks as black boxes, thus preventing contributors from specifically adapting their code to integrate and test the attack with AttackBench. Second, the output of Algorithm 2 is a readable *json* file containing all the considered metrics. Consequently, attack developers can integrate novel attacks by sharing their *json* files within the collection of benchmark results. While the runtime may not be directly comparable unless using the same hardware architecture, the optimality measure will still be valid, as it only considers the distances of the adversarial perturbations. Finally, the *optimality* measure proposed in AttackBench can be continually updated with the results of each attack efficiently. Including each new attack does not require indeed possessing data for all attacks to assess a new one; the current empirically optimal curve alone suffices. Once the results of the novel attack are uploaded, AttackBench updates the empirically optimal curve if the novel attack advances the state of the art, and refreshes the leaderboard for all attacks by recomputing Eq. 11.

IV. EXPERIMENTS

We now execute AttackBench to rate the adversarial attacks. We first detail its setup (Sect. IV-A), and we continue by discussing all the results we collected (Sect. IV-B).

A. Experimental Setup

Dataset. We set up our benchmark on two popular datasets: CIFAR-10 [37] and ImageNet [38]. We evaluate the performance of adversarial attacks on the entire test set for CIFAR-10, while considering a random subset of 5 000 samples from the validation set of ImageNet. We use a batch size of 128 for the CIFAR-10 dataset and 32 for ImageNet.

Models. We use a selection of both baseline and robust models to assess the effectiveness and adaptability of the attacks against different model architectures and defense mechanisms. For CIFAR-10, we employ five different models. The first model is an undefended WideResNet-28-10 (denoted as C1) from Robustbench [35] and is a baseline non-robust model. As for robust models, we consider the defenses from: Zhang *et al.* [39] (C2) proposing a certified defense; Stutz *et al.* [40] (C3) offering a confidence calibration method combined with adversarial training to generalize against unseen attacks;

Xiao *et al.* [41] (C4) introducing a novel activation function to enhance the model’s robustness; and Wang *et al.* [42] (C5), which combines data augmentation techniques with adversarial training. For ImageNet, we select four different models from Robustbench [35]. Specifically, we consider a pre-trained undefended ResNet-50, and three adversarially-trained models from Wong *et al.* [43] (I2), Salman *et al.* [44] (I3), and DeBenedetti [45] (I4). It is worth noting that C4 has been specifically designed to cause gradient obfuscation, and it is not robust to gradient-free attacks [9], [32]. We deliberately include this model in the evaluation to test the efficacy of the attacks under masked gradient conditions.

Adversarial Libraries. We integrate various publicly available adversarial attack libraries in AttackBench: FoolBox [46], Cleverhans [47], AdvLib [48], ART [49], TorchAttacks [50], and DeepRobust [51]. We also include the original implementations of several attacks to assess implementation inconsistencies (or improvements) among the different versions.

Attack Settings. We focus on the well-studied ℓ_p perturbation models with $p \in \{0, 1, 2, \infty\}$. We consider all the available implementations of the attacks listed in Table I, excluding FGSM [10] as it is not iterative and Biggio *et al.* [4] and Szegedy *et al.* [5] as their implementation is not available in multiple libraries. We only run the attacks in their untargeted objective, resulting in 815 tested configurations.⁵

Hyperparameters. We conduct our experiments using the default hyperparameters of both the original and library-version implementations of the attacks. We set the maximum number of forward and backward propagations to 2 000. For an attack that does a single prediction and gradient computation per optimization step, this corresponds to the common “1 000 steps budget” found in several works [18], [24], [26], [52]. Exceptionally, most implementations of the CW attack use a default number of steps equal to 10^4 for multiple runs to find c , so we modify it to perform the search of the penalty weight and the attack iterations within the 2, 000 propagations.

FixedBudget attacks, as explained in Sect. II, find the perturbation within a maximum budget ε . For these attacks, as done in [24], [29], we implement a search strategy to find the smallest budget ε^* for which the attack can successfully find an adversarial perturbation. Starting from $\varepsilon^{(0)}$, we run the attack (corresponding to one search step) and multiply (divide) ε by 2 if the attack fails (succeeds). Once the attack succeeds, we have a lower and upper bound for ε^* , so we use the remaining search steps to perform a binary search to refine the solution. In practice, we perform 10 search steps and adapt the number of attack steps to reach the overall 2 000 query budget. We use $\varepsilon^{(0)} = 100, 10, 1$, and $1/255$ for the $\ell_0, \ell_1, \ell_2, \ell_\infty$ -norm FixedBudget attacks respectively.

Evaluation Metrics. For each attack, we provide the Attack Success Rate (ASR), *i.e.* $1 - \rho(\varepsilon)$, as the percentage of samples in \mathcal{D} that the attack transforms into adversarial examples at $\varepsilon = \infty$. Additionally, we conduct a computational analysis of each attack, considering factors such as execution time and the number of forward and backward propagations required

⁵Note that APGD_t [23] executes APGD with a targeted objective against multiple candidate classes and retains the best result across trials as an untargeted solution.

for the attack. The execution time is measured on a shared compute cluster.⁶

B. Experimental Results

We present the evaluation assessments obtained with AttackBench on a total of **815** configurations. For the 5 CIFAR-10 models, we execute 6, 21, 42, and 33 attack implementations for the ℓ_0 , ℓ_1 , ℓ_2 , and ℓ_∞ threat models respectively, obtaining a total of 510 configurations. For the 4 ImageNet models, given the high data dimensionality, we reduced the load by excluding some attacks that were suboptimal in the CIFAR-10 experiment. Therefore, we execute 6, 10, 9, and 10 attacks implementations for the ℓ_0 , ℓ_1 , ℓ_2 , and ℓ_∞ threat models, obtaining 140 configurations. This wide evaluation covers the libraries and gradient-based attacks mentioned in Sect. IV-A.

Attacks Optimality Evaluation. We present in Table II the results obtained for the top-5 ranked attacks in each ℓ_p norm, according to our *GO* metric. Similarly, we report the 5 worst-performing attacks Table III. We defer to Sect. C additional results, including all the results for the other configurations included in our evaluation benchmark. We also visually depict examples of the security evaluation curves obtained with the top-ranked attacks in Fig. 3 computed against C3 [40]. We notably observe that the top-ranked attacks for the ℓ_0 (ℓ_2) threat model are σ -zero (DDN) for both CIFAR-10 and ImageNet, achieving for the latter an optimality of 99.8 (98.6). Regarding the ℓ_1 and ℓ_∞ threat models, we observe the constant presence of APGD- ℓ_1 , APGD $_t$, and PDPGD in the top 5 positions in both CIFAR-10 and ImageNet experiment. PDPGD is, for example, the top-ranked attack in ℓ_1 for CIFAR-10 and second on ImageNet by a small margin. In both cases, APGD competes with PDPGD. In ℓ_∞ , we observe that APGD $_t$ and APGD demonstrate similar results, both contending for the lead. We highlight that APGD, despite being conceived as a FixedBudget attack, offers outstanding results also when configured as a MinNorm attack. This suggests that combining APGD with the search strategy presented in Sect. IV-A is a viable strategy to efficiently find a small perturbation, even compared to MinNorm attacks. Overall, it’s noteworthy that none of the tested attacks reaches 100% of *GO*, suggesting that combining attacks can still enhance robustness evaluations obtained with single (non-optimal) attacks [35].

Fast Attacks. The top-ranked attacks Table II in terms of *GO* do not always provide the best tradeoff with efficiency. For example, in ℓ_1 , the optimality reached by APGD for ImageNet is only slightly better than that of PDPGD; however, APGD is 3× slower in its original implementation combined with the ϵ search strategy. Considering ℓ_0 , the VFGA attack is the fastest algorithm, requiring significantly fewer queries to stage the attack thanks to its early stopping mechanism. However, its ASR and *GO* largely drop for this attack when scaling to the ImageNet dataset, lessening its reliability.

Best and Worst Performing Implementation Sources. As shown in Table II, the high-ranking attacks are often implemented in AdvLib and Foolbox libraries or are directly taken

from the original repositories of the authors. Conversely, implementations from other sources, such as the Art, Cleverhans, and Deeprobust libraries, do not consistently appear among the top-performing attacks. In some cases, attacks integrated into these libraries even exhibit a decrease in performance. For example, while APGD implemented with AdvLib (as well as its original implementation) ranks high in *GO* (see Table II), its implementation from the Art library is among the worst-performing (see Table III), e.g., for CIFAR-10 under the ℓ_1 norm threat model we observe a drop in optimality from 90.9% (original implementation) to 26% (Art). Upon inspecting the code, we identified a crucial difference in the parameter controlling the number of random initializations for the attack, set to 5 in Art and to 1 in the original and AdvLib implementations. Consequently, the restart mechanism consumes available queries within the same perturbation budget, leading to early termination without exploring smaller budgets with the binary search. Another crucial difference is observed for FAB⁷ and CW⁸ because they calculate the difference of the gradients of the two logits separately, thus requiring two backward passes rather than one. A notable divergence in implementation, observable in the ImageNet results, arises between the APGD attack in the original repository and the one in the AdvLib library. In ℓ_2 (ℓ_∞), the AdvLib APGD attains a *GO* score of 95.9% (97%), whereas the original APGD yields a *GO* score of 36.2% (39.1%), highlighting a noteworthy gap of 59.7% (57.9%). While these were originally using the NCE loss, we noticed that AdvLib adopts the DLR loss by default.

Ingredients for Optimal Attacks. We here identify key elements contributing mostly to achieving a high *GO* Table II. First, we observe that almost all the listed attacks, including σ -zero, FMN, PDPGD, PGD- ℓ_0 , APGD, APGD $_t$, BIM, and DDN, leverage techniques such as normalization (Norm) or linear approximation (Proj) on the gradient, thus decoupling its original size with the choice of the step size for the update [18], [26], [29]. Remarkably, the step size schedule also appears beneficial, such as for σ -zero, FMN, PDPGD, and APGD. Examining the optimizers used by the best-performing attacks (see Table II), gradient descent (GD) emerges as the predominant choice, with occasional utilization of Adam (Adam) or momentum (GD + Mom) variants. Finally, none of the attacks securing the top rank in Table II adopts a fixed step size, confirming that dynamically reducing the step size across iterations and enhancing convergence stability contributes to achieving better optima.

Implementation Pitfalls. Through AttackBench, we observed that coding errors across diverse libraries pose significant hindrances: (i) the original BB implementation crashes if all the samples obtained with the initialization strategy are not misclassified.; (ii) TorchAttacks DeepFool fails during batch processing if a sample has a label equal to the number of classes, resulting in an index out-of-bounds error; (iii) TorchAttacks FAB ℓ_1 encounters a crash in the inner_perturb function

⁷https://github.com/fra31/auto-attack/blob/a39220048b3c9f2cca9a4d3a54604793c68eca7e/autoattack/fab_pt.py#L95

⁸<https://github.com/Trusted-AI/adversarial-robustness-toolbox/blob/0cc12f4c19f64c359aa119a1d0db14e3e064fd2e/art/attacks/evasion/carlini.py#L214>

⁶Equipped with NVIDIA V100 SXM2 GPU with 16GB of memory.

TABLE II: Top performing attacks. For each attack, we list the library implementations that offer the same or very similar results, marking in italics the best one. Also, when multiple libraries are present, we report the runtime for the attack with the best GO.

Dataset	ℓ_p	Attack	Library	ASR (%)	GO (%)	#Forwards	#Backwards	t(s)	
CIFAR-10	ℓ_0	σ -zero	Original	100	98.4	999	999	292.2	
		FMN	Original, <i>AdvLib</i>	98.7	85.3	1000	1000	278.8	
		VFGA	AdvLib	94.4	80.2	388	18	106.2	
		PGD- ℓ_0	Original	100	66.7	919	901	545.0	
		PDPGD	AdvLib	99.5	39.3	913	913	280.4	
	ℓ_1	PDPGD	AdvLib	99.8	93.2	995	995	279.6	
		APGD- ℓ_1	Original, AdvLib	100	90.9	775	755	892.4	
		FMN	Original, AdvLib, FoolBox	97.9	90.4	1000	1000	276.0	
		APGD $_t$	Original, AdvLib	100	85.4	577	536	860.6	
		EAD	FoolBox	100	70	923	923	276.7	
	ℓ_2	DDN	AdvLib, FoolBox	100	92.9	998	998	278.0	
		APGD	Original, AdvLib	100	92.9	775	755	709.2	
		APGD $_t$	Original, AdvLib	100	92.2	522	482	641.8	
		PDGD	AdvLib	99	91.7	994	994	279.6	
		FMN	Original, <i>AdvLib</i>	99.5	90.8	998	998	275.3	
	ℓ_∞	APGD $_t$	Original, AdvLib	100	97.6	629	584	626.1	
		APGD	Original, AdvLib	100	97.5	775	755	711.5	
		BIM	FoolBox	99.9	94.6	999	989	692.3	
		PGD	AdvLib	100	93.2	1000	990	281.8	
		PDPGD	AdvLib	99.8	90.8	992	992	284.6	
	ImageNet	ℓ_0	σ -zero	Original	100	99.8	999	999	345.2
			FMN	Original, <i>AdvLib</i>	100	87.5	1000	1000	358.8
			VFGA	AdvLib	63.6	71.2	928	44	76.4
			PDPGD	AdvLib	100	53.6	983	983	345.1
PGD- ℓ_0			Original	100	39.2	913	893	1680.1	
ℓ_1		APGD	Original, AdvLib	100	98	693	673	1085.9	
		PDPGD	AdvLib	100	97.3	999	999	339.2	
		APGD $_t$	Original, AdvLib	100	94.8	579	538	990.1	
		ALMA	AdvLib	100	92.5	973	973	359.3	
		EAD	FoolBox	100	90.7	403	206	77.5	
ℓ_2		DDN	AdvLib, <i>FoolBox</i>	100	98.6	1000	1000	336.0	
		APGD $_t$	AdvLib	99.9	98.1	670	650	325.1	
		BIM	FoolBox	100	97.3	1000	990	1252.4	
		FMN	Original, <i>AdvLib</i>	99.6	97.1	1000	1000	362.8	
		APGD	Original, <i>AdvLib</i>	100	95.9	1000	990	333.5	
ℓ_∞		APGD $_t$	AdvLib	99.8	99.2	718	698	358.7	
		PDPGD	AdvLib	100	98.2	987	987	409.1	
		FMN	Original, AdvLib, FoolBox	100	98.2	1000	1000	335.2	
		BIM	FoolBox	100	98	1000	990	1293.7	
		APGD	AdvLib	100	97	1000	990	334.0	

TABLE III: Worst performing attacks on CIFAR-10. For each distinct attack, we report the library name offering the lowest optimality measure. When multiple libraries are present, the runtime is reported for the emphasized one(s).

ℓ_p	Attack	Library	ASR (%)	GO (%)	#Forwards	#Backwards	t(s)
ℓ_1	PGD	FoolBox	100	55.6	1000	990	715.0
	EAD	Art	85.2	53.3	334	1665	295.7
	FGM	Art, <i>FoolBox</i>	97.7	28	40	20	30.3
	APGD	Art	98.8	25.6	822	354	456.9
	BB	FoolBox	38	38	623	36	119.4
ℓ_2	DeepFool	FoolBox	98.6	40.6	256	255	21.2
	FGM	Art, <i>Cleverhans</i> , DeepRobust, Foolbox	97.6	37.9	41	20	28.1
	DeepFool	Art	84.9	32.3	269	1341	317.8
	BB	FoolBox	38.3	30.9	624	36	112.1
	BIM	Art	95.7	22.6	808	782	322.2
ℓ_∞	APGD	Art	94.5	77.5	1037	504	390.0
	FGSM	<i>TorchAttacks</i> , FoolBox, DeepRobust, CleverHans, Art	97.6	62.9	40	20	7.9
	CW	Art, AdvLib	86.2	62.5	1321	640	2314.4
	DeepFool	Foolbox	98.3	46.8	129	128	64.1
	BB	FoolBox	42.9	32	806	135	139.0

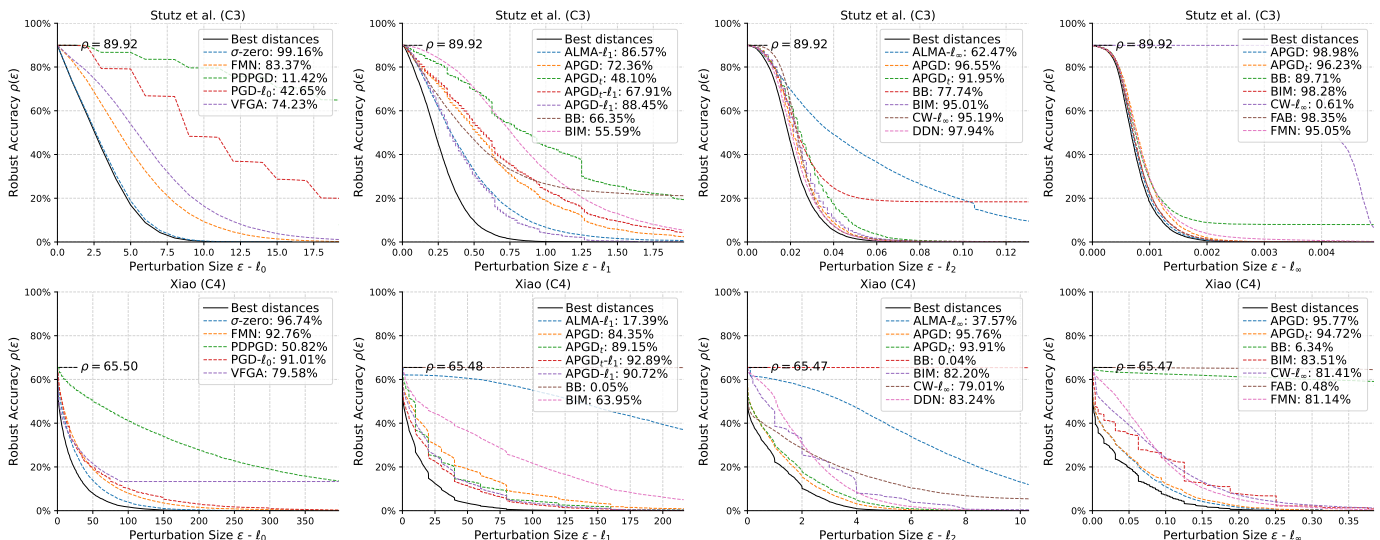


Fig. 3: Security evaluation curves for the 7 best l_0 , l_1 , l_2 , and l_∞ -norm attacks against C3 [40] (top) and C4 [41] in CIFAR-10.

due to a missing code case when the norm is neither l_2 nor l_∞ but l_1 ; (iv) ART JSMA does not provide an untargeted implementation; (v) Foolbox FMN l_0 crashes with out-of-bounds errors during the projection step. Moreover, except for AdvLib, we highlight the absence of compatibility of per-sample ϵ evaluations for FixedBudget attacks in all libraries, substantially extending their runtime.

V. RELATED WORK

We comment here on similar evaluation frameworks adopted in the state of the art by highlighting the main differences with our approach. Dong et al. [53] test the efficacy of 15 different attacks (gradient-based and gradient-free, both targeted and untargeted) on 16 robust CIFAR-10 and ImageNet models. The authors consider the performance of those at increasing perturbation budget (expressed in l_2 and l_∞ norms) and queries. Ling et al. [6] propose DeepSec, which tests 16 state-of-the-art adversarial attacks against 13 robust models on a fixed perturbation budget, analyzed through 10 and 6 metrics defined by the authors respectively. However, DeepSec has been highly criticized for its implementation flaws [54], diminishing its contribution. Croce et al. [35] propose RobustBench, a benchmark of robust models evaluated with AutoAttack [23] at a fixed perturbation budget (expressed in l_2 and l_∞ norms). Aldahdooh et al. [8] show the effectiveness of 8 adversarial examples detectors, tested with both gradient-based and gradient-free (*i.e.* black-box) attacks at selected perturbation budgets, without proposing any ranking. Guo et al. [7] propose the evaluation of robust models through 23 different metrics against several gradient-based and gradient-free attacks. It is similar to DeepSec and thus shares issues and limitations; moreover, it does not provide any model ranking.

However, all these work are limited by the issues we have shared in Sect. II-B. In particular, these solely evaluate all the possible combination of attacks and defenses, testing them with unfair settings that favor specific evaluations, on only few fixed perturbation budgets. On the contrary, thanks to the optimality

metric and to our fair setup, AttackBench stands as the only unbiased benchmark of attacks.

VI. CONCLUSION AND FUTURE WORK

In this work, we propose AttackBench, a comprehensive benchmark to evaluate gradient-based attacks. This systematic approach stands on top of a novel categorization of existing strategies, and on the optimality metric, a novel measure used to rank algorithms according to their evasive performance. We then test 102 different attack implementations, all evaluated in fair conditions that ensure both reproducibility and impartial ranking. Thanks to AttackBench, we can spotlight attacks that excel in most of the perturbation models, while also alerting the presence of critical errors of libraries that prevent some strategies from properly running.

AttackBench only supports evaluations of image classifiers, neglecting other relevant domains like image segmentation or malware detection. Nevertheless, we believe that our methodology is general enough to be easily re-casted to also match novel and diversified domains. Since we are disclosing both the models and test samples used by AttackBench, an attack might be carefully tuned on the benchmark to prevail on top of the others. For example, an attack might embed hard-coded results inside its implementation. To avoid this problem, we could implement a hidden sanity check that execute attacks on a different test set, serving as an anomaly detectors of illicit evaluations. Lastly, execution time might not be a reliable metric since it highly depends on the machine running AttackBench. However, we believe this could be easily fixed by reserving a specific service constantly running our benchmark, fairly recomputing execution time on the same machine. Also, we remark that the tracking of queries is machine-independent, thus providing a fair metric.

As future work, we will extend AttackBench not only to include targeted attacks, possible with minimal changes to the rest of the benchmark, but also to gradient-free strategies, where we would rely on forward operations only, while leaving all the other components and settings unaltered.

ACKNOWLEDGMENTS

This work has been partly supported by the EU-funded Horizon Europe projects ELSA (GA no. 101070617) and Sec4AI4Sec (GA no. 101120393); by project TESTABLE (GA no. 101019206); by project SERICS (PE00000014) under the MUR National Recovery and Resilience Plan funded by the European Union - NextGenerationEU; and by European Union—NextGenerationEU (National Sustainable Mobility Center CN00000023, Italian Ministry of University and Research Decree n. 1033—17/06/2022, Spoke 10).

REFERENCES

- [1] Antonio Brunetti, Domenico Buongiorno, Gianpaolo Francesco Trotta, and Vitoantonio Bevilacqua. Computer vision and deep learning techniques for pedestrian detection and tracking: A survey. *Neurocomputing*, 300:17–33, 2018.
- [2] Scott E Coull and Christopher Gardner. Activation analysis of a byte-based deep neural network for malware classification. In *2019 IEEE Security and Privacy Workshops (SPW)*, pages 21–27. IEEE, 2019.
- [3] Kalaivani Sundararajan and Damon L Woodard. Deep learning for biometrics: A survey. *ACM Computing Surveys*, 51(3):1–34, 2018.
- [4] B. Biggio, I. Corona, D. Maiorca, B. Nelson, N. Šrnđić, P. Laskov, G. Giacinto, and F. Roli. Evasion attacks against machine learning at test time. In *Machine Learning and Knowledge Discovery in Databases (ECML PKDD)*, volume 8190, pages 387–402, 2013.
- [5] Christian Szegedy, Wojciech Zaremba, Ilya Sutskever, Joan Bruna, Dumitru Erhan, Ian Goodfellow, and Rob Fergus. Intriguing properties of neural networks. In *Int. Conf. on Learn. Repr.*, 2014.
- [6] Xiang Ling, Shouling Ji, Jiayu Zou, Jiannan Wang, Chunming Wu, Bo Li, and Ting Wang. Deepsec: A uniform platform for security analysis of deep learning model. In *IEEE Symp. on Security and Privacy (SP)*, pages 673–690, 2019.
- [7] Jun Guo, Wei Bao, Jiakai Wang, Yuqing Ma, Xinghai Gao, Gang Xiao, Aishan Liu, Jian Dong, Xianglong Liu, and Wenjun Wu. A comprehensive evaluation framework for deep model robustness. *Pattern Recognition*, 137:109308, 2023.
- [8] Ahmed Aldahdooh, Wassim Hamidouche, Sid Ahmed Fezza, and Olivier Deforges. Adversarial example detection for dnn models: A review and experimental comparison. *Artificial Intelligence Review*, 2022.
- [9] Maura Pintor, Luca Demetrio, Angelo Sotgiu, Ambra Demontis, Nicholas Carlini, Battista Biggio, and Fabio Roli. Indicators of attack failure: Debugging and improving optimization of adversarial examples. *Advances in Neural Information Processing Systems*, 35, 2022.
- [10] Ian J. Goodfellow, Jonathon Shlens, and Christian Szegedy. Explaining and harnessing adversarial examples. In *Int. Conf. on Learn. Repr.*, 2015.
- [11] Nicolas Papernot, Patrick McDaniel, Somesh Jha, Matt Fredrikson, Z. Berkay Celik, and Ananthram Swami. The limitations of deep learning in adversarial settings. In *Proc. 1st IEEE European Symposium on Security and Privacy*, pages 372–387. IEEE, 2016.
- [12] Alexey Kurakin, Ian Goodfellow, and Samy Bengio. Adversarial examples in the physical world. *arXiv preprint arXiv:1607.02533*, 2016.
- [13] Seyed-Mohsen Moosavi-Dezfooli, Alhussein Fawzi, and Pascal Frossard. Deepfool: a simple and accurate method to fool deep neural networks. In *IEEE Conf. Computer Vision and Pattern Recognition (CVPR)*, pages 2574–2582, 2016.
- [14] Nicholas Carlini and David A. Wagner. Towards evaluating the robustness of neural networks. In *IEEE Symposium on Security and Privacy*, pages 39–57. IEEE Computer Society, 2017.
- [15] Pin-Yu Chen, Yash Sharma, Huan Zhang, Jinfeng Yi, and Cho-Jui Hsieh. Ead: elastic-net attacks to deep neural networks via adversarial examples. In *Thirty-second AAAI conference on artificial intelligence*, 2018.
- [16] A. Madry, A. Makelov, L. Schmidt, D. Tsipras, and A. Vladu. Towards deep learning models resistant to adversarial attacks. In *ICLR*, 2018.
- [17] W Brendel, J Rauber, M Kümmerer, I Ustyuzhaninov, and M Bethge. Accurate, reliable and fast robustness evaluation. In *NeurIPS*, pages 12817–12827, 2020.
- [18] Jérôme Rony, Luiz G Hafemann, Luiz S Oliveira, Ismail Ben Ayed, Robert Sabourin, and Eric Granger. Decoupling direction and norm for efficient gradient-based l2 adversarial attacks and defenses. In *IEEE/CVF Conf. on Computer Vision and Pattern Recognition*, pages 4322–4330, 2019.
- [19] Francesco Croce and Matthias Hein. Sparse and imperceptible adversarial attacks. *2019 IEEE/CVF Int. Conf. on Computer Vision (ICCV)*, pages 4723–4731, 2019.
- [20] Apostolos Modas, Seyed-Mohsen Moosavi-Dezfooli, and Pascal Frossard. Sparsefool: A few pixels make a big difference. *IEEE/CVF Conf. on Computer Vision and Pattern Recognition*, 2018.
- [21] Zhewei Yao, Amir Gholami, Peng Xu, Kurt Keutzer, and Michael W. Mahoney. Trust region based adversarial attack on neural networks. *IEEE/CVF Conf. on Computer Vision and Pattern Recognition*, pages 11342–11351, 2018.
- [22] Francesco Croce and Matthias Hein. Minimally distorted adversarial examples with a fast adaptive boundary attack. In *Int. Conf. on Machine Learning*, pages 2196–2205. PMLR, 2020.
- [23] Francesco Croce and Matthias Hein. Reliable evaluation of adversarial robustness with an ensemble of diverse parameter-free attacks. In *Int. Conf. on Machine Learning (ICML)*, 2020.
- [24] Jérôme Rony, Eric Granger, Marco Pedersoli, and Ismail Ben Ayed. Augmented lagrangian adversarial attacks. In *ICCV*, 2021.
- [25] Francesco Croce and Matthias Hein. Mind the box: l1-apgd for sparse adversarial attacks on image classifiers. In *Int. Conf. on Machine Learning*, 2021.
- [26] Maura Pintor, Fabio Roli, Wieland Brendel, and Battista Biggio. Fast minimum-norm adversarial attacks through adaptive norm constraints. In *Advances in Neural Information Processing Systems*, 2021.
- [27] Alexander Matyasko and Lap-Pui Chau. Pdpgd: Primal-dual proximal gradient descent adversarial attack. *ArXiv*, abs/2106.01538, 2021.
- [28] Hatem Hajri, Manon Césaire, Théo Combey, Sylvain Lamprier, and Patrick Gallinari. Stochastic sparse adversarial attacks. *IEEE Int. Conf. on Tools with Artificial Intelligence*, 2020.
- [29] Antonio Emanuele Cinà, Francesco Villani, Maura Pintor, Lea Schönher, Battista Biggio, and Marcello Pelillo. σ -zero: Gradient-based optimization of ℓ_0 -norm adversarial examples. *ArXiv*, 2024.
- [30] Neal Parikh, Stephen Boyd, et al. Proximal algorithms. *Foundations and trends® in Optimization*, 1(3):127–239, 2014.
- [31] Ilya Loshchilov and Frank Hutter. SGRD: stochastic gradient descent with warm restarts. In *ICLR*. OpenReview.net, 2017.
- [32] Florian Tramèr, Nicholas Carlini, Wieland Brendel, and Aleksander Madry. On adaptive attacks to adversarial example defenses. *Advances in Neural Information Processing Systems*, 33, 2020.
- [33] Battista Biggio, Giorgio Fumera, and Fabio Roli. Security evaluation of pattern classifiers under attack. *IEEE Tran. on Knowledge and Data Engineering*, 26(4):984–996, 2014.
- [34] B. Biggio and F. Roli. Wild patterns: Ten years after the rise of adversarial machine learning. *Pattern Recognition*, 84:317–331, 2018.
- [35] Francesco Croce, Maksym Andriushchenko, Vikash Sehwal, Edoardo DeBenedetti, Nicolas Flammarion, Mung Chiang, Prateek Mittal, and Matthias Hein. Robustbench: a standardized adversarial robustness benchmark. In *NeurIPS Datasets and Benchmarks*, 2021.
- [36] Quynh H. Dang. Secure hash standard (shs). 2012.
- [37] Alex Krizhevsky. Learning multiple layers of features from tiny images. 2009.
- [38] Jia Deng, Wei Dong, Richard Socher, Li-Jia Li, Kai Li, and Li Fei-Fei. Imagenet: A large-scale hierarchical image database. In *IEEE Conf. on Computer Vision and Pattern Recognition*, 2009.
- [39] Huan Zhang, Hongge Chen, Chaowei Xiao, Sven Gowal, Robert Stanforth, Bo Li, Duane Boning, and Cho-Jui Hsieh. Towards stable and efficient training of verifiably robust neural networks. In *ICLR*, 2020.
- [40] David Stutz, Matthias Hein, and Bernt Schiele. Confidence-calibrated adversarial training: Generalizing to unseen attacks. In *Int. Conf. on Machine Learning*, 2019.
- [41] Chang Xiao, Peilin Zhong, and Changxi Zheng. Enhancing adversarial defense by k-winners-take-all. In *Int. Conf. on Learn. Repr.*, *ICLR*. OpenReview.net, 2020.
- [42] Zekai Wang, Tianyu Pang, Chao Du, Min Lin, Weiwei Liu, and Shuicheng Yan. Better diffusion models further improve adversarial training. In *Int. Conf. on Machine Learning*, volume 202, pages 36246–36263, 2023.
- [43] Eric Wong, Leslie Rice, and J. Zico Kolter. Fast is better than free: Revisiting adversarial training. In *Int. Conf. on Learn. Repr.*, 2020.
- [44] Hadi Salman, Andrew Ilyas, Logan Engstrom, Ashish Kapoor, and Aleksander Madry. Do adversarially robust imagenet models transfer better? In *Advances in Neural Information Processing Systems*, 2020.
- [45] Edoardo DeBenedetti, Vikash Sehwal, and Prateek Mittal. A light recipe to train robust vision transformers. In *First IEEE Conf. on Secure and Trustworthy Machine Learning*, 2023.
- [46] Jonas Rauber, Roland Zimmermann, Matthias Bethge, and Wieland Brendel. Foolbox native: Fast adversarial attacks to benchmark the

robustness of machine learning models in pytorch, tensorflow, and jax. *Journal of Open Source Software*, 5(53):2607, 2020.

- [47] Nicolas Papernot, Fartash Faghri, Nicholas Carlini, Ian Goodfellow, Reuben Feinman, Alexey Kurakin, Cihang Xie, Yash Sharma, Tom Brown, Aurko Roy, Alexander Matyasko, Vahid Behzadan, Karen Hambardzumyan, Zhishuai Zhang, Yi-Lin Juang, Zhi Li, Ryan Sheatsley, Abhibhav Garg, Jonathan Uesato, Willi Gierke, Yinpeng Dong, David Berthelot, Paul Hendricks, Jonas Rauber, and Rujun Long. Cleverhans v2.1.0. *arXiv*, 2018.
- [48] Jérôme Rony and Ismail Ben Ayed. Adversarial Library.
- [49] Maria-Irina Nicolae, Mathieu Sinn, Minh-Ngoc Tran, Beat Buesser, Ambrish Rawat, Martin Wistuba, Valentina Zantedeschi, Nathalie Baracaldo, Bryant Chen, Heiko Ludwig, Ian Molloy, and Ben Edwards. Adversarial robustness toolbox v1.0.0. *arXiv*, 2018.
- [50] Hoki Kim. Torchattacks : A pytorch repository for adversarial attacks. *ArXiv*, abs/2010.01950, 2020.
- [51] Yaxin Li, Wei Jin, Han Xu, and Jiliang Tang. Deeprobust: A pytorch library for adversarial attacks and defenses. *arXiv*, 2020.
- [52] Wieland Brendel, Jonas Rauber, and Matthias Bethge. Decision-based adversarial attacks: Reliable attacks against black-box machine learning models. In *Int. Conf. on Learn. Repr.*, 2018.
- [53] Yinpeng Dong, Qi-An Fu, Xiao Yang, Tianyu Pang, Hang Su, Zihao Xiao, and Jun Zhu. Benchmarking adversarial robustness on image classification. In *2020 IEEE/CVF Conf. on Computer Vision and Pattern Recognition*, pages 318–328, 2020.
- [54] Nicholas Carlini. A critique of the deepsec platform for security analysis of deep learning models, 2019.
- [55] Nicholas Carlini, Matthew Jagielski, Christopher A Choquette-Choo, Daniel Paleka, Will Pearce, Hyrum Anderson, Andreas Terzis, Kurt Thomas, and Florian Tramèr. Poisoning web-scale training datasets is practical. *arXiv*, 2023.

Antonio Emanuele Cinà (MSc 2019, PhD 2023) is an Assistant Professor at the University of Genoa, Italy. His research interests focus on the security of AI systems and the study of their trustworthiness. In particular, he has studied possible vulnerabilities and emerging risks arising from AI caused by the malicious use training data. Finally, he works in the field of Generative AI, exploring how this technology can be integrated to optimise user applications.



Jérôme Rony is a machine learning scientist at Synlico Inc. working on computational biology. He received his PhD from ÉTS Montréal in 2023, where his research focused on solving constrained optimization problems involving neural networks, which are central to designing safe and trustworthy models.



Maura Pintor is an Assistant Professor at the PRA Lab, in the Department of Electrical and Electronic Engineering of the University of Cagliari, Italy. She received her PhD in Electronic and Computer Engineering from the University of Cagliari in 2022. Her research focuses on machine learning security, with a particular focus on optimizing and debugging adversarial attacks.



Luca Demetrio (MSc 2017, PhD 2021) is an Assistant Professor at the University of Genoa. He is currently studying the security of Windows malware detectors implemented with Machine Learning techniques, and he is first author of papers published in top-tier journals (ACM TOPS, IEEE TIFS). He is part of the development team of SecML, and the maintainer of SecML Malware, a Python library for creating adversarial Windows malware.



Ambra Demontis is an Assistant Professor at the University of Cagliari, Italy. She received her M.Sc. degree (Hons.) in Computer Science and her Ph.D. degree in Electronic Engineering and Computer Science from the University of Cagliari, Italy. Her research interests include secure machine learning, kernel methods, biometrics, and computer security.



Battista Biggio (MSc 2006, PhD 2010) is Full Professor at the University of Cagliari, Italy, and co-founder of the company Pluribus One. His research interests include adversarial machine learning and cybersecurity. He is the recipient of the 2022 ICML Test of Time Award, for his work on “Poisoning Attacks against Support Vector Machines”. He is Senior Member of the IEEE and of the ACM, and Member of the IAPR and ELLIS.



Ismail Ben Ayed is currently a full professor with ÉTS Montréal and affiliated with the CRCHUM. His interests are in computer vision, optimization, machine learning and medical image analysis algorithms. He authored more than 100 peer-reviewed papers, mostly published in the top venues, along with 2 books and 7 U.S. patents. His research has been covered in several visible media outlets, such as Radio Canada (CBC), Quebec Science Magazine and Canal du Savoir. His research team received several recent distinctions, such as the MIDL'19 best paper runner-up award and several top-ranking positions in internationally visible contests. He served on the program committee for MICCAI'15, '17, and '19 and as program chair for MIDL'20. He regularly serves as a reviewer for the main scientific journals of his field, and was selected several times among the top reviewers of prestigious conferences (such as CVPR'15 and NeurIPS'20).



Fabio Roli is a Full Professor of Computer Science at the University of Genoa, Italy. He has been appointed Fellow of the IEEE and Fellow of the International Association for Pattern Recognition. He is a recipient of the Pierre Devijver Award for his contributions to statistical pattern recognition.

APPENDIX

A. Samples Hashing

AttackBench uses the SHA-512 hashing algorithm, standardized by NIST [36], to associate each sample with a unique compressed representation for accurately tracking and identifying samples throughout the benchmarking process. The choice of SHA-512 is motivated by its cryptographic strength and resistance to collisions. Also, the choice of sample hashing seamlessly solve the problem of evaluating attacks on the same set of samples. Controversy, one common strategy for evaluating attacks is to use the entire testing set of widely-used datasets (like CIFAR-10), but this could be challenging and unnecessary, especially when considering large-scale datasets such as ImageNet. Thus, researchers often expedite comparisons by relying on arbitrary data subsets [26], difficult to reconstruct without curated metadata (*e.g.* the indexes of the samples used). Moreover, the content of these datasets may undergo alterations over time [55], potentially compromising the integrity of the comparison. Thus, we must guarantee that future evaluations will consider the same subset or content to establish a common and unique baseline. Another trivial solution would be sharing the samples used during the evaluations, but this would expose us to the risk of potential license infringements. Thus, AttackBench employs a hashing algorithm to associate each sample with a unique compressed representation, significantly reducing the risk of sample replacement and collaterally containing the size of saved information, facilitating result sharing.

B. Optimality Score Development

The development of this measure involves a structured three-step process, highlighted in Algorithm 3. Firstly, we subject a target model to an exhaustive range of attacks $\{a^1, \dots, a^N\}$, recording the minimum best distances d^* required to render each sample adversarial (line 2). We then use the collected distances to construct an empirically derived curve $\rho_{\theta}^*(\epsilon)$, which effectively captures the model’s optimal trade-off between robustness and perturbation size, for the best empirical attack a^* (line 3). This curve maps the minimum perturbation generated by the array of attacks for every validation sample. Finally, we to quantitatively assess the *optimality* of a specific attack, we propose calculating the difference in the areas under the curves obtained from the empirically derived curve and the curve generated by the attack under evaluation (line 5).

C. Additional Experiments

In the following, we report the results that, for space constraints, we have not reported in the paper. In particular, we show the security evaluation curves, the top-5 $\ell - \text{inf}$ performing attacks on CIFAR-10, and the tables showing the local optimality for all the considered implementations run on CIFAR-10. Upon request, we can add the same tables for ImageNet.

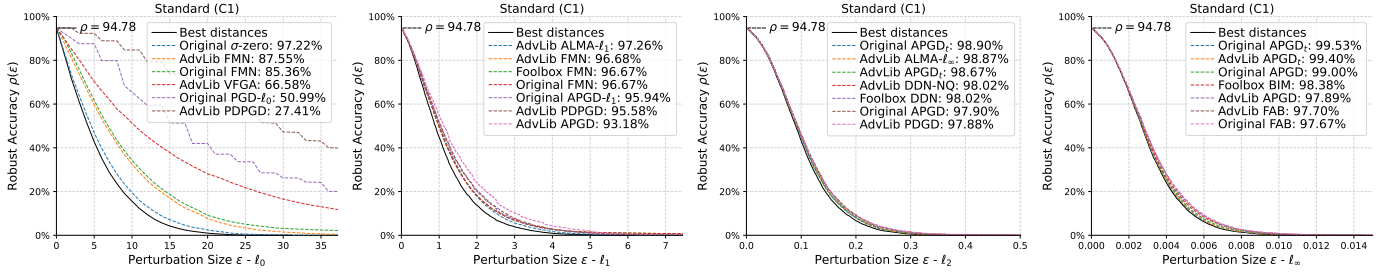


Fig. 4: Security evaluation curves for the best l_0 , l_1 , l_2 , and l_∞ -norm attacks against C1 in CIFAR-10.

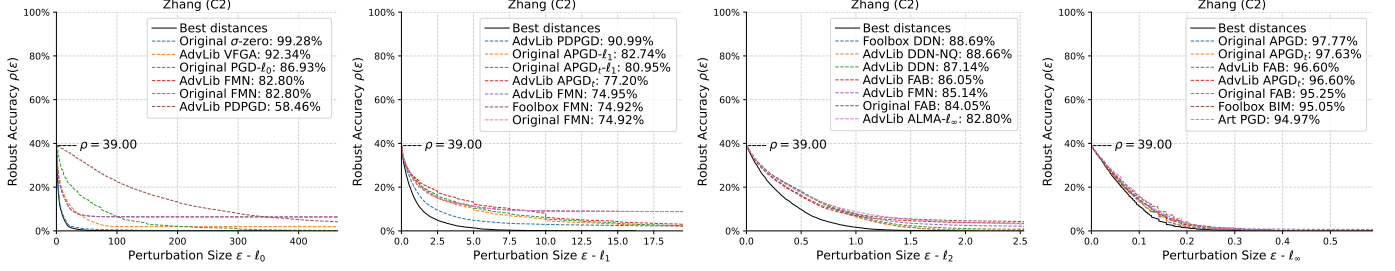


Fig. 5: Security evaluation curves for the best l_p -norm attacks against C2 in CIFAR-10.

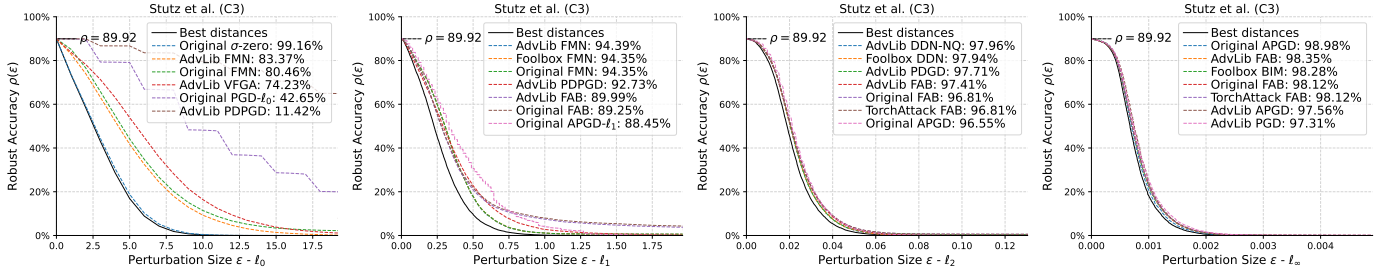


Fig. 6: Security evaluation curves for the best l_p -norm attacks against C3 in CIFAR-10.

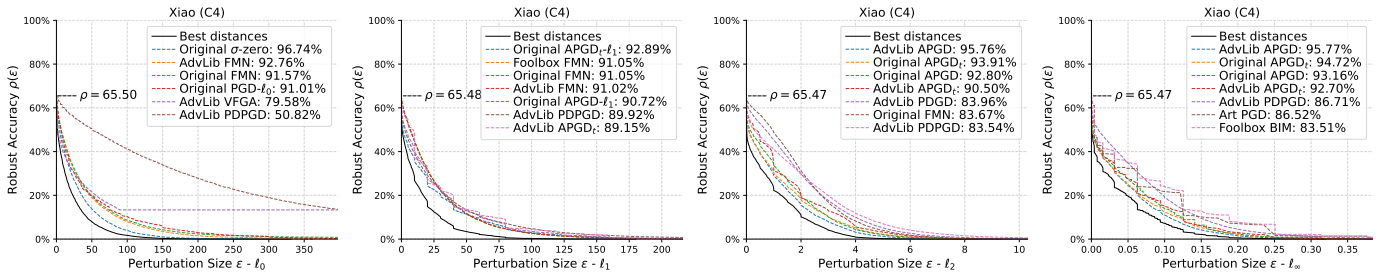


Fig. 7: Security evaluation curves for the best l_p -norm attacks against C4 in CIFAR-10.

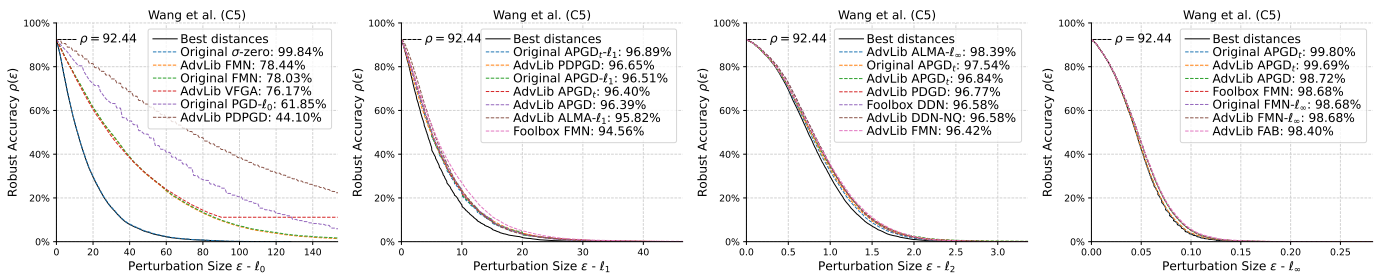


Fig. 8: Security evaluation curves for the best l_p -norm attacks against C5 in CIFAR-10.

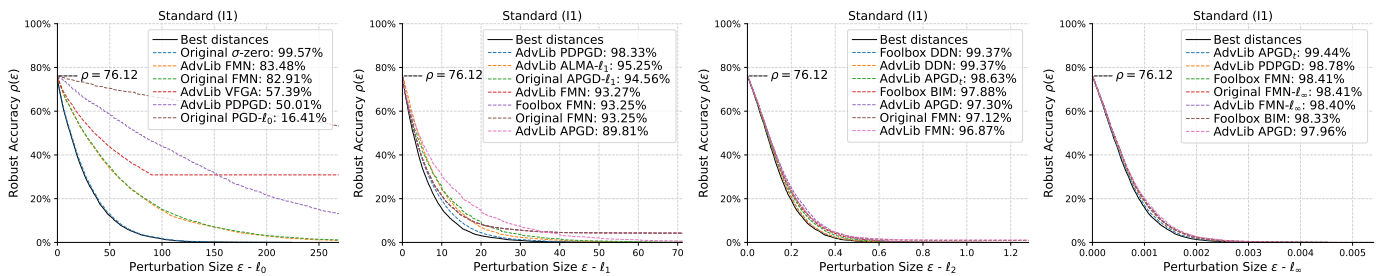


Fig. 9: Security evaluation curves for the best ℓ_p -norm attacks against I1 in ImageNet.

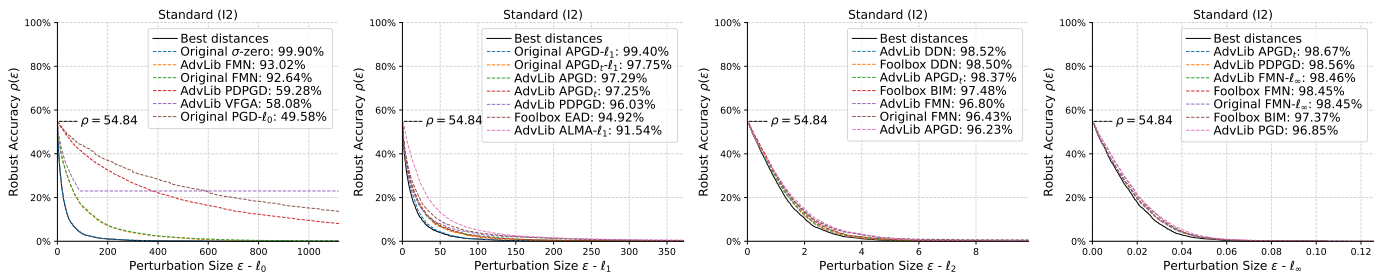


Fig. 10: Security evaluation curves for the best ℓ_p -norm attacks against I2 in ImageNet.

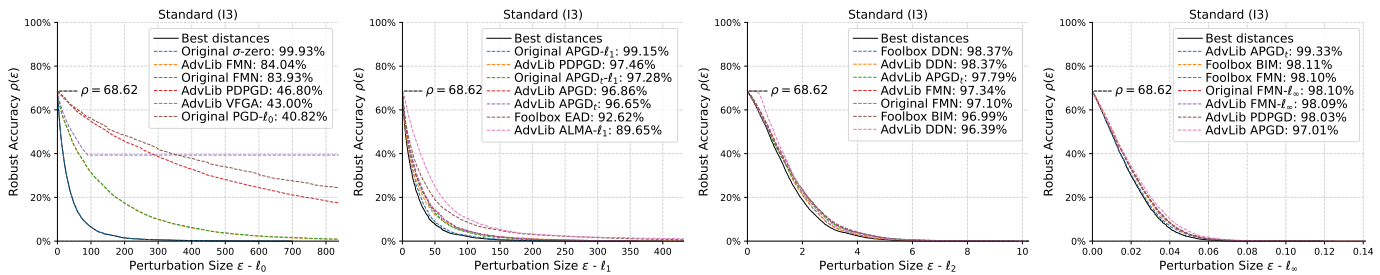


Fig. 11: Security evaluation curves for the best ℓ_p -norm attacks against I3 in ImageNet.

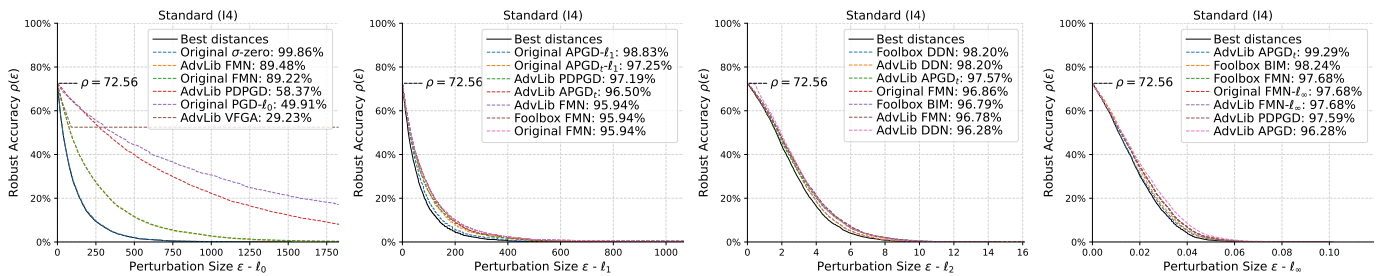


Fig. 12: Security evaluation curves for the best ℓ_p -norm attacks against I4 in ImageNet.

TABLE IV: Top ℓ_∞ -norm performing attacks with batch size equals to 1. For each attack, we list the library implementations that offer the same or very similar results. When multiple libraries are present, the runtime is reported for the emphasized one.

Dataset	ℓ_p	Attack	Library	ASR (%)	Optimality (%)	#Forwards	#Backwards	t(s)
CIFAR-10	ℓ_∞	APGD	TorchAttacks, Original, AdvLib	100	98.5	802	782	10.0
		APGD $_t$	Original, AdvLib	100	97.7	626	581	8.8
		BIM	FoolBox	100	95.1	1000	990	10.2
		PDPGD	AdvLib	99.8	94.6	1000	1000	12.4
		PGD	AdvLib, FoolBox	100	93.6	1000	990	10.0

TABLE V: Local optimality for ℓ_0 -norm attacks.

Model	Attack	ASR	Optimality	#Forwards	#Backwards	ExecTime
C1	Original σ -zero	100	97.2	999	999	269.7
	AdvLib FMN	100	87.5	1000	1000	266.6
	Original FMN	100	85.4	892	892	264.5
	AdvLib VFGA	98.7	66.9	359	17	50.9
	Original PGD- ℓ_0	100	51	974	955	423.5
	AdvLibPDPGD	100	28.4	839	838	264.6
C2	Original σ -zero	100	99.3	998	998	4.3
	AdvLib VFGA	98	94.3	183	8	1.3
	Original PGD- ℓ_0	100	86.9	812	794	69.4
	AdvLib FMN	93.6	84.5	1000	1000	3.4
	Original FMN	93.6	84.5	999	999	4.8
	AdvLibPDPGD	97.9	58.5	997	997	5.0
C3	Original σ -zero	100	99.2	999	999	38.5
	AdvLib FMN	100	83.4	1000	1000	37.6
	Original FMN	100	80.5	842	842	40.9
	AdvLib VFGA	100	74.2	136	6	3.1
	Original PGD- ℓ_0	100	42.6	953	934	134.6
	AdvLibPDPGD	100	14.5	848	848	40.0
C4	Original σ -zero	100	96.7	999	999	46.3
	AdvLib FMN	100	92.8	999	999	45.5
	Original FMN	99.8	91.6	690	690	47.3
	Original PGD- ℓ_0	100	91	880	861	286.1
	AdvLib VFGA	86.7	87.5	496	23	15.5
	AdvLibPDPGD	99.7	50.9	919	919	47.2
C5	Original σ -zero	100	99.8	999	999	292.2
	AdvLib FMN	100	78.4	999	999	278.8
	AdvLib VFGA	88.8	78.2	768	36	106.2
	Original FMN	100	78	911	911	277.3
	Original PGD- ℓ_0	100	61.8	978	959	545.0
	AdvLibPDPGD	99.9	44.2	962	962	280.4

TABLE VI: Local optimality for ℓ_1 -norm attacks.

Model	Attack	ASR	Optimality	#Forwards	#Backwards	ExecTime
C1	AdvLib ALMA	100	97	993	993	262.9
	AdvLib FMN	99	97	1,000	1,000	268.7
	FoolBox FMN	99	97	1,000	1,000	265.8
	Original FMN	99	97	1,000	1,000	264.3
	Original APGD- ℓ_1	100	96	958	938	523.0
	AdvLib PDPGD	100	96	992	992	263.3
	AdvLib APGD	100	93	1,000	990	274.9
	Original APGD $_t$	100	88	667	622	546.6
	AdvLib APGD $_t$	100	87	590	570	160.8
	AdvLib FAB	95	83	361	1,620	267.5
	Original FAB	94	83	311	1,544	255.8
	FoolBox EAD	100	82	405	207	80.5
	Art EAD	100	73	334	1,665	275.2
	TorchAttacks FAB	5	61	311	1,544	256.9
	Art PGD	84	48	1,010	980	579.3
	FoolBox PGD	100	47	1,000	990	640.9
	FoolBox BIM	100	46	220	200	284.4
	FoolBox FGSM	99	26	40	20	30.3
	Art FGSM	99	26	40	20	31.5
	FoolBox BB	5	24	634	0	96.7
Art APGD	100	12	1,044	457	456.9	
C2	AdvLib PDPGD	99	91	997	997	5.2
	Original APGD- ℓ_1	100	83	406	386	144.0
	Original APGD $_t$	100	81	306	275	163.4
	AdvLib APGD $_t$	100	77	637	617	12.7
	AdvLib FMN	91	75	1,000	1,000	4.0
	FoolBox FMN	91	75	1,000	1,000	5.1
	Original FMN	91	75	1,000	1,000	5.3
	AdvLib FAB	98	74	360	1,619	3.7
	Original FAB	97	71	128	635	2.9
	FoolBox BIM	100	67	220	200	21.2
	Art PGD	84	66	1,010	980	35.4
	FoolBox EAD	100	61	355	182	1.0
	FoolBox PGD	100	60	999	989	57.0
	AdvLib APGD	100	59	999	989	11.0
	AdvLib ALMA	100	55	841	841	5.4
	TorchAttacks FAB	61	54	128	635	2.9
	Art FGSM	98	48	40	20	2.3
	FoolBox FGSM	98	48	40	20	2.2
	Art EAD	79	41	334	1,665	6.4
	Art APGD	100	33	441	179	38.0
FoolBox BB	61	17	637	0	1.9	
C4	Original APGD $_t$	100	93	558	518	526.8
	FoolBox FMN	100	91	999	999	48.0
	Original FMN	100	91	999	999	46.7
	AdvLib FMN	100	91	1,000	1,000	46.1
	Original APGD- ℓ_1	100	91	668	648	547.5
	AdvLib PDPGD	100	90	998	998	46.9
	AdvLib APGD $_t$	100	89	690	670	43.8
	AdvLib APGD	100	84	998	988	53.0
	FoolBox EAD	100	83	292	150	10.6
	FoolBox BIM	100	64	220	200	160.1
	FoolBox PGD	100	61	999	989	317.4
	Art PGD	42	58	1,010	980	169.8
	TorchAttacks FAB	35	54	155	790	31.9
	Art EAD	47	38	334	1,665	44.5
	Art APGD	100	37	773	331	228.8
	Art FGSM	99	34	40	20	18.4
	FoolBox FGSM	99	34	40	20	16.8
	AdvLib ALMA	100	17	805	805	47.9
	Original FAB	92	10	155	790	32.2
	FoolBox BB	35	7	629	0	20.8
AdvLib FAB	96	2	216	1,012	41.4	

TABLE VII: Local optimality for ℓ_1 -norm attacks (pt2).

Model	Attack	ASR	Optimality	#Forwards	#Backwards	ExecTime
C5	Original APGD _t	100	97	726	679	860.6
	AdvLib PDPGD	100	97	998	998	279.6
	Original APGD- ℓ_1	100	97	935	915	892.4
	AdvLib APGD _t	100	96	657	637	190.5
	AdvLib APGD	100	96	1,000	990	284.2
	AdvLib ALMA	100	96	989	989	276.7
	FoolBox FMN	100	95	1,000	1,000	281.2
	Original FMN	100	95	1,000	1,000	276.0
	AdvLib FMN	100	95	1,000	1,000	276.7
	AdvLib FAB	98	88	360	1,618	288.1
	FoolBox EAD	100	86	482	245	96.5
	Original FAB	96	85	303	1,505	268.3
	TorchAttacks FAB	8	59	303	1,505	275.6
	Art EAD	100	58	334	1,665	295.7
	Art PGD	24	55	1,010	980	429.7
	FoolBox PGD	100	52	1,000	990	715.0
	FoolBox BIM	100	49	220	200	279.2
	Art FGSM	93	22	40	20	29.5
	FoolBox FGSM	93	22	40	20	27.5
	FoolBox BB	9	5	647	2	119.4
Art APGD	94	3	1,098	482	303.2	
C3	AdvLib FMN	99	94	1,000	1,000	38.9
	FoolBox FMN	99	94	1,000	1,000	39.0
	Original FMN	99	94	1,000	1,000	39.5
	AdvLib PDPGD	100	93	992	992	39.0
	AdvLib FAB	97	90	361	1,620	38.9
	Original FAB	97	89	295	1,465	33.8
	Original APGD- ℓ_1	100	89	910	890	133.9
	AdvLib ALMA	100	87	987	987	39.5
	AdvLib APGD	100	72	1,000	990	44.8
	Art PGD	100	69	1,010	980	127.2
	Original APGD _t	100	68	628	584	231.2
	FoolBox BB	81	66	567	176	51.7
	TorchAttacks FAB	10	60	295	1,465	33.2
	FoolBox PGD	100	58	1,000	990	135.1
	Art EAD	100	57	334	1,665	42.6
	FoolBox BIM	100	56	220	200	137.2
	AdvLib APGD _t	100	48	572	552	32.8
	FoolBox EAD	100	48	389	199	10.9
	Art APGD	100	42	752	321	253.6
	Art FGSM	100	11	40	20	19.0
FoolBox FGSM	100	11	40	20	17.5	

TABLE VIII: Local optimality for ℓ_2 -norm attacks (pt1).

Model	Attack	ASR	Optimality	#Forwards	#Backwards	ExecTime
C2	FoolBox DDN	100	88.7	999	999	3.7
	AdvLib DDN-NQ	100	88.7	999	999	3.6
	AdvLib DDN	99.3	87.2	1000	1000	3.2
	TorchAttacks FAB	92.2	86.8	128	635	3.2
	AdvLib FAB	99	86.1	360	1618	3.6
	AdvLib FMN	98.1	85.2	998	998	3.4
	Original FAB	98.2	84.1	128	635	2.9
	AdvLib ALMA	100	82.8	993	993	5.6
	AdvLib PDGD	95	82.3	1000	1000	3.4
	Original APGD	100	81.1	406	386	74.4
	Original APGD _t	100	78.6	317	285	85.1
	AdvLib APGD _t	99.8	78.1	720	700	4.7
	Original FMN	92.1	74.7	1000	1000	4.6
	FoolBox BIM	99.8	71.5	1000	990	62.9
	AdvLib APGD	100	70.6	999	989	4.1
	AdvLib TrustRegion	77.9	70.2	356	187	3.0
	Original TrustRegion	77.9	70.2	841	187	3.7
	TorchAttacks PGD	99.9	68.9	998	988	53.4
	Art PGD	87.3	63.9	1010	980	50.4
	DeepRobust PGD	66.3	62.7	1186	777	10.4
	FoolBox PGD	100	60.6	999	989	61.6
	TorchAttacks CW	73.1	60.3	379	379	1.4
	TorchAttacks APGD	61	59.6	1	0	0.0
	Art APGD	99.9	59	412	165	53.7
	FoolBox CW	99.6	58.3	784	784	3.4
	AdvLib CW	88.1	58.2	846	845	3.2
	Original DeepFool	83.9	58	7	51	8.1
	FoolBox DeepFool	92.8	57.6	998	997	3.3
	AdvLib PDPGD	99.1	54.9	984	984	5.0
	Original TrustRegion	77.7	50	743	132	3.5
	AdvLib TrustRegion	77.7	50	370	132	2.7
	Art CW	71.5	46.6	485	1514	9.8
	FoolBox FGSM	98.2	45.6	40	20	2.1
	Cleverhans FGSM	98.2	45.6	41	20	2.1
	Art FGSM	98.2	45.6	40	20	2.2
	DeepRobust FGSM	97.6	45.1	39	19	2.2
	Art DeepFool	78.8	44.9	334	1666	29.0
	Cleverhans CW	76.3	44	1000	1000	23.4
	FoolBox BB	61.1	40.9	637	0	1.9
	FoolBox FMN	93.8	34.8	1000	1000	4.4
AdvLib PGD	99.5	19.5	996	986	3.0	
Art BIM	98.8	13.6	833	807	34.1	

TABLE IX: Local optimality for ℓ_2 -norm attacks (pt2).

Model	Attack	ASR	Optimality	#Forwards	#Backwards	ExecTime
C4	AdvLib APGD	100	95.8	999	989	45.8
	Original APGD _t	100	93.9	509	468	398.5
	Original APGD	100	92.8	668	648	406.5
	AdvLib APGD _t	99.3	90.5	613	593	33.0
	AdvLib PDGD	100	84	997	997	46.2
	Original FMN	100	83.7	999	999	47.4
	AdvLib PDPGD	100	83.5	979	979	47.3
	FoolBox DDN	100	83.2	992	992	46.6
	AdvLib DDN	100	83.2	992	992	46.7
	AdvLib DDN-NQ	100	83.2	992	992	45.4
	FoolBox BIM	99.8	82.2	995	985	413.0
	AdvLib FMN	100	81.2	994	994	45.6
	TorchAttacks PGD	99.4	80.3	996	986	421.2
	AdvLib CW	94.8	79	921	920	42.7
	AdvLib TrustRegion	58.8	73.4	612	315	26.6
	Original TrustRegion	58.8	73.4	969	315	35.9
	Art PGD	84.7	72.3	1010	980	423.0
	FoolBox PGD	99.7	70.6	996	986	402.4
	AdvLib PGD	99.3	70.1	997	987	44.6
	TorchAttacks CW	51.4	69.3	163	163	7.5
	FoolBox CW	99.3	67.3	301	301	14.3
	DeepRobust PGD	48.2	66.6	1184	776	95.7
	Cleverhans CW	59.8	61.2	1000	1000	65.6
	Art CW	36.9	58	480	1519	53.3
	FoolBox FMN	100	57.9	438	438	47.0
	TorchAttacks APGD	34.5	56.1	1	0	0.0
	Art APGD	99.7	52.8	708	300	291.2
	TorchAttacks FAB	34.6	50	85	453	32.7
	AdvLib TrustRegion	55	44.8	732	253	27.6
	Original TrustRegion	55.1	44.5	984	253	34.6
	Art BIM	94.3	40.4	720	696	218.9
	FoolBox FGSM	99.1	38.6	40	20	17.5
	DeepRobust FGSM	99.1	38.6	40	20	19.3
	Art FGSM	99.1	37.8	40	20	18.6
	Cleverhans FGSM	99.1	37.8	41	20	17.8
	AdvLib ALMA	100	37.6	978	978	47.3
	FoolBox BB	34.6	4.3	630	0	20.4
	Original FAB	93.6	1.4	85	453	31.9
	AdvLib FAB	98.2	1.2	125	617	41.6
	Original DeepFool	91.9	1.2	4	20	19.4
FoolBox DeepFool	100	0.9	51	50	2.3	
Art DeepFool	92.6	0.8	12	63	1.7	

TABLE X: Local optimality for ℓ_2 -norm attacks (pt3).

Model	Attack	ASR	Optimality	#Forwards	#Backwards	ExecTime
C3	AdvLib DDN-NQ	100	98	1000	1000	37.4
	FoolBox DDN	100	97.9	1000	1000	37.8
	AdvLib PDGD	100	97.7	991	991	38.5
	AdvLib FAB	100	97.4	361	1620	38.8
	Original FAB	99.5	96.8	295	1465	33.0
	TorchAttacks FAB	99.5	96.8	295	1465	33.2
	Original APGD	100	96.6	910	890	61.9
	Art APGD	100	95.7	557	236	49.2
	Cleverhans CW	100	95.2	1000	1000	57.5
	FoolBox BIM	100	95	1000	990	64.7
	AdvLib APGD	100	94.9	1000	990	38.0
	Original FMN	99.9	93.9	1000	1000	38.6
	AdvLib FMN	99.9	93.7	1000	1000	38.0
	Original APGD _t	100	92	514	474	64.6
	AdvLib APGD _t	98.6	90.4	493	473	21.5
	Art CW	99.4	88.6	478	1521	48.6
	FoolBox PGD	100	87.3	1000	990	73.0
	Art PGD	100	86.6	1010	980	76.7
	AdvLib PDPGD	100	82.7	928	928	40.1
	AdvLib DDN	100	82.4	1000	1000	37.5
	AdvLib CW	100	81.3	999	999	38.7
	AdvLib TrustRegion	100	79.6	92	55	4.8
	Original TrustRegion	100	79.6	243	55	7.2
	FoolBox BB	81.6	78.5	571	178	17.5
	TorchAttacks PGD	100	77.1	1000	990	92.5
	FoolBox CW	100	77	616	616	24.1
	AdvLib PGD	100	75.9	1000	990	37.4
	Original TrustRegion	100	74	68	23	2.1
	AdvLib TrustRegion	100	74	42	23	1.7
	AdvLib ALMA	100	62.5	997	997	39.1
	FoolBox FMN	100	62.4	730	730	39.5
	TorchAttacks APGD	10.1	62.4	1	0	0.0
	DeepRobust PGD	41.4	45.2	1183	774	83.5
	TorchAttacks CW	100	44.8	230	230	8.9
	FoolBox DeepFool	100	27.1	91	90	3.4
	Original DeepFool	95.5	27.1	4	24	20.0
	Art FGSM	100	25.6	40	20	17.7
	FoolBox FGSM	100	25.6	40	20	16.8
	DeepRobust FGSM	100	25.6	40	20	17.9
	Cleverhans FGSM	100	25.6	41	20	17.0
	Art DeepFool	80.6	19.8	334	1666	66.7
	Art BIM	93.2	0.7	803	777	75.2

TABLE XI: Local optimality for ℓ_2 -norm attacks (pt4).

Model	Attack	ASR	Optimality	#Forwards	#Backwards	ExecTime
C1	Original APGD _t	100	98.9	579	536	319.2
	AdvLib ALMA	100	98.9	999	999	262.2
	AdvLib APGD _t	99.6	98.7	524	504	136.9
	AdvLib DDN-NQ	100	98	1000	1000	261.5
	FoolBox DDN	100	98	1000	1000	262.3
	Original APGD	100	97.9	958	938	396.7
	AdvLib PDGD	100	97.9	988	988	266.3
	Original FMN	99.6	97.6	1000	1000	267.5
	AdvLib FMN	99.6	97.5	1000	1000	262.3
	FoolBox BIM	100	97.4	1000	990	402.4
	AdvLib FAB	100	96.9	361	1620	270.2
	Original FAB	100	96.8	311	1544	255.2
	TorchAttacks FAB	100	96.8	311	1544	256.7
	AdvLib APGD	100	96.8	1000	990	263.1
	Art PGD	100	96.1	1010	980	428.7
	AdvLib CW	100	96	999	999	261.5
	FoolBox CW	100	95.8	780	780	209.5
	Art APGD	100	95.8	698	297	289.0
	Cleverhans CW	100	95.5	1000	1000	282.2
	TorchAttacks PGD	100	93.9	1000	990	408.7
	FoolBox PGD	100	93.6	1000	990	433.9
	AdvLib DDN	100	93.3	1000	1000	259.9
	AdvLib PDPGD	100	90.1	940	940	265.2
	AdvLib TrustRegion	99.6	89.1	265	141	58.9
	Original TrustRegion	99.6	89.1	731	141	118.0
	AdvLib TrustRegion	100	87.6	54	27	11.1
	Original TrustRegion	100	87.6	77	27	13.7
	Art CW	99.5	84.8	475	1524	284.3
	AdvLib PGD	100	78.5	1000	990	260.3
	FoolBox DeepFool	100	67.2	81	80	21.2
	Original DeepFool	96.3	67.2	4	24	32.9
	FoolBox FMN	100	66.2	938	938	266.6
	TorchAttacks APGD	5.2	66.2	1	0	0.1
	TorchAttacks CW	100	65.3	201	201	52.9
	DeepRobust PGD	21.1	51.4	1181	773	318.7
	Art DeepFool	78.1	47.9	334	1666	296.9
	DeepRobust FGSM	98.6	45.5	40	20	31.6
	FoolBox FGSM	98.6	45.5	40	20	31.6
	Art FGSM	98.6	45.1	40	20	29.3
	Cleverhans FGSM	98.6	44.3	41	20	27.6
Art BIM	93	34.2	813	788	274.3	
FoolBox BB	5.4	26.5	634	0	95.9	

TABLE XII: Local optimality for ℓ_2 -norm attacks (pt5).

Model	Attack	ASR	Optimality	#Forwards	#Backwards	ExecTime
C5	AdvLib ALMA	100	98.4	999	999	280.7
	Original APGD _t	100	97.5	693	645	641.8
	AdvLib APGD _t	99.9	96.8	641	621	183.6
	AdvLib PDGD	100	96.8	996	996	279.6
	FoolBox DDN	100	96.6	999	999	278.3
	AdvLib DDN-NQ	100	96.6	999	999	278.0
	AdvLib FMN	100	96.4	999	999	275.3
	Original FMN	100	96.4	1000	1000	280.4
	AdvLib DDN	100	96.3	999	999	280.3
	Original APGD	100	96	935	915	709.2
	AdvLib APGD	100	95.7	1000	990	277.3
	AdvLib FAB	100	95.6	360	1619	287.6
	Cleverhans CW	99.2	95.5	1000	1000	298.8
	FoolBox BIM	100	95.3	1000	990	707.8
	TorchAttacks PGD	100	94.9	1000	990	812.3
	FoolBox CW	100	94.4	771	771	215.0
	AdvLib CW	99.9	94.4	801	799	222.2
	Original FAB	98.4	93.6	304	1506	271.7
	Art PGD	99.9	93.3	1010	980	764.9
	FoolBox PGD	100	86.4	1000	990	728.9
	TorchAttacks FAB	61.9	84.9	304	1506	269.9
	TorchAttacks CW	72.9	84.4	553	553	152.0
	Original TrustRegion	37.5	74.7	1190	536	235.8
	AdvLib TrustRegion	37.5	74.7	1053	536	221.0
	TorchAttacks APGD	7.6	70.9	1	0	0.1
	Art CW	61.2	68.8	476	1523	307.3
	AdvLib PDPGD	100	68.5	979	979	281.5
	DeepRobust PGD	9.5	67.6	1005	657	261.5
	Original TrustRegion	38.6	59.1	1201	361	207.8
	AdvLib TrustRegion	38.6	59.1	1056	361	198.4
	Art APGD	99.3	54.3	945	411	583.1
	FoolBox DeepFool	100	50	57	56	15.7
	Original DeepFool	94.9	50	3	19	24.6
	Art DeepFool	94.5	48.1	329	1643	317.8
	FoolBox FMN	100	48	809	809	277.0
	Cleverhans FGSM	92.3	36	41	20	28.1
	Art FGSM	92.3	36	40	20	29.8
	FoolBox FGSM	92.3	35.9	40	20	27.9
	DeepRobust FGSM	92.3	35.9	40	20	29.4
	AdvLib PGD	100	29.4	999	989	274.3
	Art BIM	99.1	23.8	869	841	322.2
	FoolBox BB	8.6	4.3	646	2	112.1

TABLE XIII: Local optimality for ℓ_∞ -norm attacks.

Model	Attack	ASR	Optimality	#Forwards	#Backwards	ExecTime
C4	AdvLib APGD	100	95.8	1000	990	45.6
	Original APGD _t	100	94.7	572	529	295.4
	Original APGD	100	93.2	668	648	306.1
	AdvLib APGD _t	98.6	92.7	723	703	37.3
	AdvLib PDPGD	100	86.7	979	979	50.7
	Art PGD	99.5	86.6	1006	976	272.3
	FoolBox BIM	99.7	83.5	996	986	273.7
	AdvLib PGD	100	81.9	999	989	44.5
	DeppRobust PGD	99.5	81.7	1007	987	255.5
	AdvLib CW	99.8	81.4	594	594	36.8
	FoolBoxFMN	100	81.1	996	996	46.2
	Original FMN	100	81.1	996	996	46.4
	AdvLib FMN	100	81.1	996	996	45.5
	TorchAttacks PGD	99.4	80.9	996	986	253.3
	FoolBox PGD	99.6	76	997	987	271.1
	Art APGD	89	76	902	434	185.0
	Original TrustRegion	99.3	64.2	944	104	35.6
	AdvLib TrustRegion	99.3	64.1	191	104	18.1
	Original TrustRegion	97	62.2	1127	89	42.2
	AdvLib TrustRegion	96.9	62.1	239	89	20.9
	Art CW	63.4	57.9	1324	645	1893.7
	Art BB	34.5	56.4	13	0	12.1
	TorchAttacks APGD	34.5	56.4	1	0	0.0
	TorchAttacks FGSM	97.4	51.8	40	20	1.4
	Art FGSM	97.4	51.8	40	20	16.3
	Cleverhans FGSM	97.4	51.8	41	20	14.5
	DeppRobust FGSM	97.4	51.8	40	20	18.4
	FoolBox FGSM	97.4	51.8	40	20	15.6
	FoolBox BB	42.8	6.6	717	0	26.1
	TorchAttacks FAB	35.1	4.3	80	501	32.6
	FoolBox DeepFool	91.8	0.9	396	394	64.1
	Original FAB	97.4	0.8	80	501	32.9
	AdvLib FAB	99.9	0.6	126	726	42.0

TABLE XIV: Local optimality for ℓ_∞ -norm attacks (pt2).

Model	Attack	ASR	Optimality	#Forwards	#Backwards	ExecTime
C2	Original APGD	100	97.8	406	386	34.2
	Original APGD _t	100	97.6	373	338	40.9
	AdvLib FAB	99.9	96.6	362	1627	4.0
	AdvLib APGD _t	99.8	96.6	930	910	5.0
	TorchAttacks FAB	98.7	95.5	131	647	3.2
	Original FAB	99.3	95.4	131	647	3.1
	FoolBox BIM	100	95.1	999	989	28.6
	Art PGD	100	95	1009	979	35.1
	DeppRobust PGD	100	94.7	1009	989	30.8
	TorchAttacks PGD	100	94.5	999	989	29.5
	AdvLib PGD	100	94.2	999	989	2.8
	FoolBox PGD	100	93.4	999	989	28.3
	AdvLib APGD	100	90.8	999	989	4.4
	AdvLib PDPGD	99.1	88.4	890	890	8.5
	Original TrustRegion	99.6	88.1	689	55	3.1
	AdvLib TrustRegion	99.6	88.1	92	55	2.8
	Original TrustRegion	98.7	86.6	901	32	4.8
	AdvLib TrustRegion	98.7	86.6	70	32	3.4
	Art FGSM	99	84.1	40	20	2.0
	Cleverhans FGSM	99	84.1	41	20	1.7
	DeppRobust FGSM	99	84.1	40	20	2.1
	FoolBox FGSM	99	84.1	40	20	1.8
	TorchAttacks FGSM	99	84.1	40	20	0.1
	FoolBoxFMN	97.3	80	984	984	4.9
	Original FMN	97.3	80	984	984	4.8
	AdvLib FMN	97.3	80	984	984	3.7
	FoolBox DeepFool	99.9	79.5	101	100	0.5
	AdvLib CW	95.9	77	402	402	5.6
	Art CW	78.5	69.2	1311	636	392.2
	Art APGD	95.1	62	555	264	50.8
	Art BB	61	59.2	13	0	2.2
	TorchAttacks APGD	61	59.2	1	0	0.0
	FoolBox BB	61.1	39.3	743	0	2.2

TABLE XV: Local optimality for ℓ_∞ -norm attacks (pt3).

Model	Attack	ASR	Optimality	#Forwards	#Backwards	ExecTime
C3	Original APGD	100	99	910	890	197.7
	AdvLib FAB	100	98.4	363	1629	39.2
	FoolBox BIM	100	98.3	1000	990	210.8
	Original FAB	99.9	98.1	301	1492	33.6
	TorchAttacks FAB	99.9	98.1	301	1492	34.0
	AdvLib APGD	100	97.6	1000	990	37.8
	AdvLib PGD	100	97.3	1000	990	37.1
	FoolBox PGD	100	96.5	1000	990	202.6
	Original APGD _t	100	96.2	680	633	260.5
	AdvLib APGD _t	99	95.5	644	624	27.9
	AdvLib FMN	100	95.1	1000	1000	37.7
	FoolBoxFMN	100	95.1	1000	1000	38.4
	Original FMN	100	95.1	1000	1000	38.5
	Art APGD	100	92.6	1212	590	122.8
	FoolBox BB	92	90.7	1038	634	133.0
	AdvLib PDPGD	100	87.8	872	872	42.6
	DeppRobust PGD	100	85.4	1010	990	319.6
	Art PGD	100	85.3	1010	980	326.2
	TorchAttacks PGD	100	85.1	1000	990	284.6
	Original TrustRegion	100	77.6	13	12	0.5
	AdvLib TrustRegion	100	77.6	8	12	0.5
	Original TrustRegion	100	77.5	10	12	0.5
	AdvLib TrustRegion	100	77.5	6	12	0.4
	TorchAttacks FGSM	100	62.1	40	20	1.1
	Art FGSM	100	62.1	40	20	18.0
	Cleverhans FGSM	100	62.1	41	20	17.3
	DeppRobust FGSM	100	62.1	40	20	18.4
	FoolBox FGSM	100	62.1	40	20	16.9
	Art CW	99.7	61.7	1291	622	1393.2
	TorchAttacks APGD	10.1	61.7	1	0	0.0
	FoolBox DeepFool	100	27	37	36	1.4
	Art BB	13.7	0.7	20	3	11.2
	AdvLib CW	100	0.6	307	306	17.6

TABLE XVI: Local optimality for ℓ_∞ -norm attacks (pt4).

Model	Attack	ASR	Optimality	#Forwards	#Backwards	ExecTime
C1	Original APGD _t	100	99.5	707	659	626.1
	AdvLib APGD _t	99.7	99.4	641	621	169.1
	Original APGD	100	99	958	938	711.5
	FoolBox BIM	100	98.4	1000	990	692.3
	AdvLib APGD	100	97.9	1000	990	263.7
	AdvLib FAB	100	97.7	363	1629	268.1
	Original FAB	100	97.7	317	1573	262.1
	TorchAttacks FAB	100	97.7	317	1573	257.9
	FoolBoxFMN	100	97	1000	1000	262.8
	Original FMN	100	97	1000	1000	264.4
	AdvLib FMN	100	96.9	1000	1000	271.2
	AdvLib PGD	100	96.9	1000	990	260.9
	AdvLib PDPGD	100	96.4	970	970	269.7
	FoolBox PGD	100	95.4	1000	990	727.3
	Art APGD	99.7	93.2	1274	623	390.0
	TorchAttacks PGD	100	88.6	1000	990	696.4
	DeppRobust PGD	100	86	1010	990	707.0
	AdvLib TrustRegion	100	84.9	10	14	3.5
	Original TrustRegion	100	84.9	24	14	5.2
	AdvLib TrustRegion	100	83.8	12	13	3.5
	Original TrustRegion	100	83.8	19	13	4.4
	Art PGD	100	77.4	1010	980	798.6
	FoolBox DeepFool	100	67	48	47	12.9
	TorchAttacks APGD	5.2	66	1	0	0.2
	AdvLib CW	100	61	758	756	206.6
	TorchAttacks FGSM	99.8	56.2	40	20	7.8
	Art FGSM	99.8	56.2	40	20	31.7
	Cleverhans FGSM	99.8	56.2	41	20	30.5
	DeppRobust FGSM	99.8	56.2	40	20	31.9
	FoolBox FGSM	99.8	56.2	40	20	30.2
	Art CW	100	42.3	1346	651	2269.6
	FoolBox BB	7.7	3.9	751	17	110.9
	Art BB	10.3	0.5	24	5	29.0

TABLE XVII: Local optimality for ℓ_∞ -norm attacks (pt5).

Model	Attack	ASR	Optimality	#Forwards	#Backwards	ExecTime
C5	Original APGD _t	100	99.8	813	760	416.0
	AdvLib APGD _t	99.8	99.7	783	763	223.0
	AdvLib APGD	100	98.7	1000	990	278.2
	FoolBoxFMN	100	98.7	999	999	279.8
	Original FMN	100	98.7	999	999	277.2
	AdvLib FMN	100	98.7	999	999	275.2
	AdvLib FAB	100	98.4	362	1628	289.2
	Original APGD	100	98.4	935	915	446.6
	FoolBox BIM	100	98	1000	990	451.0
	DeppRobust PGD	100	97.9	1010	990	453.6
	TorchAttacks PGD	100	97.8	1000	990	449.0
	Art PGD	100	96.8	1010	980	474.3
	Original FAB	98.3	96.6	309	1534	273.5
	TorchAttacks FAB	98.3	96.6	309	1534	274.8
	AdvLib PGD	100	95.9	1000	990	281.8
	AdvLib CW	100	94.9	911	911	264.6
	AdvLib PDPGD	100	94.9	899	899	284.6
	FoolBox PGD	100	94.6	1000	990	450.4
	AdvLib TrustRegion	100	92.1	108	63	26.6
	Original TrustRegion	100	92.1	279	63	47.8
	AdvLib TrustRegion	100	91.4	42	23	9.7
	Original TrustRegion	100	91.4	68	23	12.7
	Art CW	89.5	81.1	1331	648	2314.4
	Art APGD	88.8	63.5	1243	611	367.1
	Art BB	7.6	63.2	21	0	20.6
	TorchAttacks APGD	7.6	63.2	1	0	0.2
	TorchAttacks FGSM	91.7	60.3	40	20	7.9
	Art FGSM	91.7	60.3	40	20	25.0
	Cleverhans FGSM	91.7	60.3	41	20	24.1
	DeppRobust FGSM	91.7	60.3	40	20	24.9
	FoolBox FGSM	91.7	60.3	40	20	23.8
	FoolBox DeepFool	100	59.7	62	61	17.4
	FoolBox BB	10.9	19.3	782	23	139.0